Article

Hypochlorite-Mediated Fragmentation of Hyaluronan, Chondroitin Sulfates, and Related *N*-Acetyl Glycosamines: Evidence for Chloramide Intermediates, Free Radical Transfer Reactions, and Site-Specific Fragmentation

Martin D. Rees, Clare L. Hawkins, and Michael J. Davies

J. Am. Chem. Soc., **2003**, 125 (45), 13719-13733• DOI: 10.1021/ja0370591 • Publication Date (Web): 18 October 2003

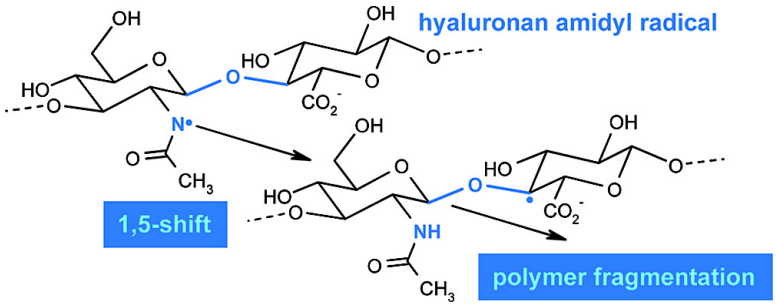

More About This Article

Additional resources and features associated with this article are available within the HTML version:

- Supporting Information
- Links to the 2 articles that cite this article, as of the time of this article download
- Access to high resolution figures
- Links to articles and content related to this article
- Copyright permission to reproduce figures and/or text from this article

View the Full Text HTML

J|A|C|S
ARTICLES
Published on Web 10/18/2003

Hypochlorite-Mediated Fragmentation of Hyaluronan, Chondroitin Sulfates, and Related *N*-Acetyl Glycosamines: Evidence for Chloramide Intermediates, Free Radical Transfer Reactions, and Site-Specific Fragmentation

Martin D. Rees, Clare L. Hawkins, and Michael J. Davies*

Contribution from the Heart Research Institute, 145 Missenden Road, Camperdown, Sydney NSW 2050, Australia

Received July 3, 2003; E-mail: m.davies@hri.org.au

Abstract: Myeloperoxidase released from activated phagocytes reacts with H_2O_2 in the presence of chloride ions to give hypochlorous acid. This oxidant has been implicated in the fragmentation of glycosaminoglycans, such as hyaluronan and chondroitin sulfates. In this study it is shown that reaction of HOCl with glycosaminoglycans and model compounds yields chloramides derived from the *N*-acetyl function of the glycosamine rings. The results of EPR spin trapping and product studies are consistent with the formation of amidyl radicals from these chloramides via both metal ion-dependent and -independent processes. In the case of glycosaminoglycan-derived amidyl radicals, evidence has been obtained in studies with model glycosides that these radicals undergo rapid intramolecular abstraction reactions to give carbon-centered radicals at C-2 on the *N*-acetyl glycosamine rings (via a 1,2-hydrogen atom shift) and at C-4 on the neighboring uronic acid residues (via 1,5-hydrogen atom shifts). The C-4 carbon-centered radicals, and analogous species derived from model glycosides, undergo pH-independent β-scission reactions that result in glycosidic bond cleavage. With *N*-acetyl glucosamine C-1 alkyl glycosides, product formation via this mechanism is near quantitative with respect to chloramide loss. Analogous reactions with the glycosaminoglycans result in selective fragmentation at disaccharide intervals, as evidenced by the formation of "ladders" on gels; this selectivity is less marked under atmospheric oxygen concentrations than under anoxic conditions, due to competing peroxyl radical reactions. As the extracellular matrix plays a key role in mediating cell adhesion, growth, activation, and signaling, such HOCl-mediated glycosaminoglycan fragmentation may play a key role in disease progression and resolution, with the resulting fragments modulating the magnitude and quality of the immune response in inflammatory conditions.

Introduction

Activated phagocytes release the heme enzyme myeloperoxidase (MPO) and also generate H_2O_2 via an oxidative burst.[1] Reaction of MPO with H_2O_2 in the presence of chloride ions generates a mixture of hypochlorous acid and its anion (pK_a 7.59[2]);[3] HOCl is used henceforth to designate this mixture. HOCl is a potent bactericide and plays an important role in mammalian defenses against invading microorganisms.[4] However, there is now considerable evidence that excessive or misplaced generation of HOCl may play a role in the development of a number of human inflammatory diseases including atherosclerosis, rheumatoid arthritis, periodontal disease, proteinuric glomerulopathies, and some cancers.[3,5−8] The reaction of HOCl with amine or amide groups on proteins, DNA and glycosaminoglycans has been shown to produce macromolecule-derived chloramines (RNHCl) and chloramides (RNClC(O)R′).[9−13] These species have been postulated to play a role in the damage induced by HOCl as a result of their catalyzed, or spontaneous, decomposition to (nitrogen-centered) aminyl (RNH$^\bullet$) and amidyl (RN$^\bullet$-C(O)R′) radicals, respectively.[10,11]

Glycosaminoglycans are linear polysaccharides with a disaccharide repeat-unit structure consisting (typically) of a glycosamine residue (glucosamine or galactosamine) and a uronic acid residue (glucuronic or iduronic acids). The glycosamine residue in these repeat-unit structures is usually *N*-acetylated or *N*-sulfated and, with the exception of hyaluronan, glycosaminoglycans also contain *O*-sulfated residues. Due to the presence of the carboxylate and/or sulfate functions, glycosaminoglycans are negatively charged overall. As myeloperoxidase is a highly basic protein, this enzyme binds electrostatically to matrix glycosaminoglycans.[14,15] Metal ions

(1) Weiss, S. J.; LoBuglio, A. F. *Lab. Invest.* **1982**, *47*, 5−18.
(2) Morris, J. C. *J. Phys. Chem.* **1966**, *70*, 3798−3805.
(3) Kettle, A. J.; Winterbourn, C. C. *Redox Rep.* **1997**, *3*, 3−15.
(4) Thomas, E. L. *Infect. Immun.* **1979**, *23*, 522−531.
(5) Thomas, E. L.; Grisham, M. B.; Jefferson, M. M. *Methods Enzymol.* **1986**, *132*, 585−593.
(6) Waddington, R. J.; Moseley, R.; Embery, G. *Oral Dis.* **2000**, *6*, 138−151.
(7) Winterbourn, C. C.; Kettle, A. J. *Free Radical Biol. Med.* **2000**, *29*, 403−409.
(8) Grone, H. J.; Grone, E. F.; Malle, E. *Lab. Invest.* **2002**, *82*, 5−14.
(9) Weiss, S. J.; Lampert, M. B.; Test, S. T. *Science* **1983**, *222*, 625−628.
(10) Hawkins, C. L.; Davies, M. J. *Biochem. J.* **1998**, *332*, 617−625.
(11) Hawkins, C. L.; Davies, M. J. *Free Radical Biol. Med.* **1998**, *24*, 1396−1410.
(12) Prutz, W. A. *Arch. Biochem. Biophys.* **1996**, *332*, 110−120.
(13) Hawkins, C. L.; Davies, M. J. *Chem. Res. Toxicol.* **2002**, *14*, 1071−1081.

Chart 1. Glycosaminoglycans and Model Compound Structures[a]

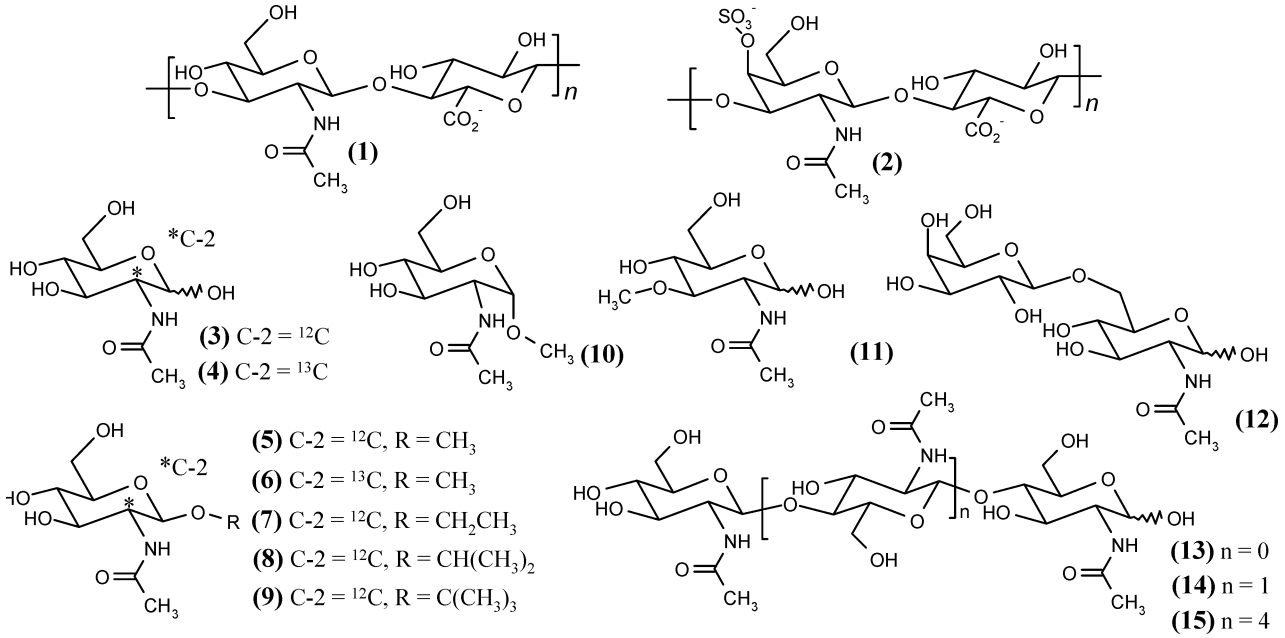

[a] (**1**): *hyaluronan*, [4)-*β*-D-Glc*p*A-(1→3)-*β*-D-Glc*p*NAc-(1→]$_n$; (**2**): *chondroitin-4-sulfate*, [4)-*β*-D-Glc*p*A-(1→3)-*β*-D-Gal*p*NAc4S -(1→]$_n$ (the sample used had a ratio of 4:1 of chondroitin-4-sulfate to chondroitin-6-sulfate according to the manufacturers); (**3**): *N-acetyl glucosamine*, 2-acetamido-2-deoxy-D-glucopyranose; (**4**): *N-acetyl [2-^{13}C]-glucosamine*, [2-^{13}C]-2-acetamido-2-deoxy-D-glucopyranose; (**5**): *β-methyl glycoside*, methyl 2-acetamido-2-deoxy-*β*-D-glucopyranoside; (**6**): *[2-^{13}C]-β-methyl glycoside*, methyl [2-^{13}C]-2-acetamido-2-deoxy-*β*-D-glucopyranoside; (**7**): *β-ethyl glycoside*, ethyl 2-acetamido-2-deoxy-*β*-D-glucopyranoside; (**8**): *β-isopropyl glycoside*, isopropyl 2-acetamido-2-deoxy-*β*-D-glucopyranoside; (**9**): *β-tert-butyl glycoside*, *tert*-butyl 2-acetamido-2-deoxy-*β*-D-glucopyranoside; (**10**): α-*methyl glycoside*, methyl 2-acetamido-2-deoxy-α-D-glucopyranoside; (**11**): 2-acetamido-2-deoxy-3-*O*-methyl-D-glucopyranoside; (**12**): *N-acetyl allolactosamine*, *β*-D-Gal*p*-(1→6)-*β*-D-Glc*p*NAc (**13**): *di-N-acetyl chitobiose*, *β*-D-Glc*p*NAc-(1→4)-D-Glc*p*NAc; (**14**): *tri-N-acetyl chitotriose*. *β*-D-Glc*p*NAc-(1→4)-*β*-D-Glc*p*NAc-(1→4)-D-Glc*p*NAc; (**15**): *hexa-N-acetyl chitohexaose*, *β*-D-Glc*p*NAc-(1→4)-*β*-D-Glc*p*NAc-(1→4)-*β*-D-Glc*p*NAc-(1→4)-*β*-D-Glc*p*NAc-(1→4)-*β*-D-Glc*p*NAc-(1→4)-*β*-D-Glc*p*NAc.

also bind to these materials,[16] and elevated levels of metal ions have been detected at sites of inflammation and macromolecule degradation.[17,18] Glycosaminoglycan modification may be of considerable biological significance, as the extracellular matrix plays a key role in modulating the behavior of cells (reviewed in ref 19). Low-molecular-mass hyaluronan oligosaccharides are known to modify macrophage expression of chemokines, cytokines, and growth factors, as well as cell-surface markers,[20−24] and can attenuate the proliferation of endothelial, fibroblast, and smooth muscle cells.[25] Hyaluronan molecules of lower molecular mass accumulate at sites of inflammation and tissue injury[23,26−28] as do modified/fragmented versions of other matrix components including chondrotin sulfates[29−31] and proteins.[32] How these materials arise is unclear, with both the action of hyaluronidase[33] and nonenzymatic oxidant-mediated processes, such as those mediated by myeloperoxidase, being potential sources.

It has been shown that the myeloperoxidase-generated oxidant HOCl reacts with glycosamine sugars at the *N*-acetyl function to generate long-lived *N*-chloramides,[11] that decomposition of polymer-derived *N*-chloro species promoted by one-electron reductants can lead to the formation of polymer-derived carbon-centered radicals (detected via EPR spin trapping),[11] and that these reactions result in polymer fragmentation.[11,34−37] These observations are consistent with polymer-derived amidyl and carbon-centered radicals being important intermediates in the fragmentation process; however, the nature of the intermediate radicals and the mechanism of fragmentation have not been unequivocably established.

In the study reported here, the role of 1,2-, 1,5-, and 1,6-hydrogen atom abstraction reactions initiated by amidyl radicals

(14) McGowan, S. E. *Am. J. Respir. Cell Mol. Biol.* **1990**, *2*, 271−279.
(15) Hazell, L. J.; Arnold, L.; Flowers, D.; Waeg, G.; Malle, E.; Stocker, R. *J. Clin. Invest.* **1996**, *97*, 1535−1544.
(16) Barbucci, R.; Magnani, A.; Lamponi, S.; Mitola, S.; Ziche, M.; Morbidelli, L.; Bussolino, F. *J. Inorg. Biochem.* **2000**, *81*, 229−237.
(17) Yuan, X. M.; Brunk, U. T. *APMIS* **1998**, *106*, 825−842.
(18) Sayre, L. M.; Perry, G.; Harris, P. L.; Liu, Y.; Schubert, K. A.; Smith, M. A. *J. Neurochem.* **2000**, *74*, 270−279.
(19) Raines, E. W. *Int. J. Exp. Pathol.* **2000**, *81*, 173−182.
(20) Noble, P. W.; Lake, F. R.; Henson, P. M.; Riches, D. W. *J. Clin. Invest.* **1993**, *91*, 2368−2377.
(21) Horton, M. R.; McKee, C. M.; Bao, C.; Liao, F.; Farber, J. M.; Hodge-DuFour, J.; Pure, E.; Oliver, B. L.; Wright, T. M.; Noble, P. W. *J. Biol. Chem.* **1998**, *273*, 35088−35094.
(22) Horton, M. R.; Boodoo, S.; Powell, J. D. *J. Biol. Chem.* **2002**, *277*, 43757−43762.
(23) McKee, C. M.; Penno, M. B.; Cowman, M.; Burdick, M. D.; Strieter, R. M.; Bao, C.; Noble, P. W. *J. Clin. Invest.* **1996**, *98*, 2403−2413.
(24) McKee, C. M.; Lowenstein, C. J.; Horton, M. R.; Wu, J.; Bao, C.; Chin, B. Y.; Choi, A. M.; Noble, P. W. *J. Biol. Chem.* **1997**, *272*, 8013−8018.
(25) West, D. C.; Kumar, S. *Exp. Cell. Res.* **1989**, *183*, 179−196.
(26) Balazs, E. A.; Watson, D.; Duff, I. F.; Roseman, S. *Arthritis Rheum.* **1967**, *10*, 357−376.
(27) Bjermer, L.; Lundgren, R.; Hallgren, R. *Thorax* **1989**, *44*, 126−131.
(28) Horton, M. R.; Burdick, M. D.; Strieter, R. M.; Bao, C.; Noble, P. W. *J. Immunol.* **1998**, *160*, 3023−3030.
(29) Kramsch, D. M.; Hollander, W. *J. Clin. Invest.* **1973**, *52*, 236−247.
(30) Kramsch, D. M.; Franzblau, C.; Hollander, W. *Adv. Exp. Med. Biol.* **1974**, *43*, 193−210.
(31) Wagner, W. D.; Salisbury, B. G. J.; Rowe, H. A. *Arteriosclerosis* **1987**, *6*, 407−417.
(32) Woods, A.; Linton, S. M.; Davies, M. J. *Biochem. J.* **2003**, *370*, 729−735.
(33) Lokeshwar, V. B.; Iida, N.; Bourguignon, L. Y. *J. Biol. Chem.* **1996**, *271*, 23853−23864.
(34) Saari, H.; Konttinen, Y. T.; Friman, C.; Sorsa, T. *Inflammation* **1993**, *17*, 403−415.
(35) Schiller, J.; Arnhold, J.; Arnold, K. *Z. Naturforsch.* **1995**, *50C*, 721−728.
(36) Schiller, J.; Arnhold, J.; Zachaus, A.; Arnold, K. *Z. Naturforsch.* **1997**, *52C*, 694−701.
(37) Jahn, M.; Baynes, J. W.; Spiteller, G. *Carbohydr. Res.* **1999**, *321*, 228−234.

in the HOCl-mediated decomposition of glycosaminoglycans and related *N*-acetyl glycosamine derivatives (Chart 1) has been examined. While alkoxyl and aminyl radicals readily undergo remote 1,5-hydrogen atom abstraction reactions,[38] structural, electronic, and solvent effects can result in the occurrence of other intramolecular processes including 1,2- and 1,6-shifts.[38] A 1,2-hydrogen atom shift reaction of amidyl radicals has been postulated to account for the generation of α-carbon-centered radicals from peptide-derived amidyl radicals in aqueous solution,[39] but unambiguous evidence for this process is lacking. It is shown here that intramolecular rearrangement reactions play an important role in site-selective fragmentation of glycosaminoglycans induced by HOCl.

Results

Reaction of *N*-acetyl glucosamine and related compounds (Chart 1; 9.1 or 83 mM in amides) with HOCl (0.45 or 8.3 mM) at pH 7.4 and 37 °C resulted in the loss of the optical absorption band of $^{-}$OCl at 292 nm and the generation of new chromophore with $\lambda_{max} < 220$ nm assigned to the *N*-chloramide (RNClC(O)R′).[11,40] The presence of good isobestic points is consistent with the formation of this single chromophoric product. After reaction was complete, chloramide formation was quantified, with respect to HOCl added, by assay using 5-thio-2-nitrobenzoic acid (TNB); yields were typically greater than 75%. The resulting chloramides were stored at 4 °C until use and were not characterized further.

Reactions of hyaluronan (3.65 mg/mL; ca. 9.1 mM in amides) and chondroitin-4-sulfate (4.6 mg/mL; ca. 9.0 mM in amides) with HOCl were examined in a similar manner. With HOCl (0.455 mM) complex multiphase kinetics were detected with complete consumption of HOCl occurring within 8 h. Chloramide formation was quantified by removal of aliquots from the reaction mixture, with these subjected to size-exclusion chromatography on PD10 columns. The polymer-containing fractions were subsequently assayed using TNB. Polymer chloramides were detected at increasing concentrations to a maximal level at 6 h, consistent with the time course of HOCl consumption. At this time point, the chloramide yields were ca. 22% (chondroitin-4-sulfate) and 29% (hyaluronan) with respect to HOCl added.

With higher concentrations of HOCl (4.55 mM), loss of the $^{-}$OCl absorption was accompanied by the generation of a new absorption band with $\lambda_{max} < 220$ nm. The presence of good isobestic points in these reactions is consistent with the formation of single chromophoric products assigned to the polymer chloramides. HOCl consumption was incomplete after 7 h under these conditions.

High yields of polymer-derived chloramides, in the absence of residual HOCl, were obtained by subjecting the treated polymers to size-exclusion (PD10) chromatography (as above) after reaction with HOCl (45.5 mM) for 16 min at 37 °C. Under such conditions, the polymers coeluted with TNB-reactive material in the high-molecular-mass fractions, and without significant decrease in molecular mass as determined by PAGE analysis (results not shown). This approach reproducibly yielded chloramide concentrations, as assayed by TNB, of ca. 0.7 and 1.6 mM for chondroitin-4-sulfate and hyaluronan, respectively, representing ca. 16% and ca. 35% conversion of the polymer *N*-acetyl amide functions to chloramides.

Incubation of hyaluronan (ca. 9.1 mM in amides) or chondroitin-4-sulfate (ca. 9.0 mM in amides) with MPO (20 nM heme) in the presence of H_2O_2 (6 × 80 μM aliquots at 10 min intervals) and 100 mM NaCl at 37 °C and pH 7.4 for 60 min led to the generation of high-molecular-mass chloramides as assayed by TNB following isolation of the high-molecular-mass material by size-exclusion (PD10) chromatography. These species coeluted with the intact polysaccharides and were not detected in the absence of the polysaccharides, nor in the absence of the MPO cosubstrates H_2O_2 or Cl^-. The concentrations of chloramides generated in these reactions were ca. 2 μM for hyaluronan and ca. 12 μM for chondroitin-4-sulfate after accounting for dilution during the chromatography. These low yields are attributed to the rapid inactivation of MPO by H_2O_2.[41]

Chloramide decomposition was examined at 37 °C and pH 7.4 in the presence and absence of added reagents (Figure 1). In the absence of added agents, the alkyl glycoside chloramides were long-lived under both aerobic and anoxic conditions, whereas those from *N*-acetyl glucosamine and related oligosaccharides showed significant decomposition over 24 h (Figure 1A). With the polysaccharide-derived chloramides, negligible decomposition occurred over 24 h at 37 °C under aerobic conditions (Figure 1, B,C), whereas at 50 °C significant decomposition occurred over 24 h (data not shown). Samples kept at 4 °C showed little decomposition over 24 h (data not shown).

The presence of a range of metal ions resulted in an enhanced rate of chloramide decomposition. Exposure of polymer chloramides to Cu^{2+} (10 nM to 100 μM) at 37 °C and pH 7.4 resulted in an enhanced rate of chloramide loss, which was time-, O_2-, and concentration-dependent (Figure 1, B−E). With 500 nM Cu^{2+} at 37 °C and pH 7.4 under aerobic conditions polymer chloramide decomposition was complete after 6 h (Figure 1, B,C); under anoxic conditions decomposition was complete within 2 h (Figure 1E). Similar behavior was detected with hyaluronan (data not shown). Inclusion of EDTA (500 nM), SOD (196 units/mL; 0.05 mg/mL), and BSA (0.05 mg/mL) in aerobic incubations resulted in a significant decrease in the rate of chloramide decomposition (Figure 1F; similar behavior was detected with hyaluronan, data not shown). The action of SOD was unaffected by the absence of O_2, suggesting that this protection is a nonspecific, protein-mediated effect, consistent with the protection afforded by BSA. Inclusion of Fe^{3+}, or Fe^{3+}-EDTA (1:1 complex) at 37 °C and pH 7.4 under aerobic conditions did not enhance the rate of polymer chloramide decomposition over 24 h. EDTA alone had no effect.

Exposure of the chloramides of *N*-acetyl glucosamine, di-*N*-acetyl-chitobiose and the C-1 alkyl glycosides to Cu^{2+} at 37 °C and pH 7.4 also resulted in an enhanced rate of chloramide decomposition (data not shown). As with the polymer chloramides, the rate of the Cu^{2+}-induced decomposition of these chloramides was more rapid in the absence of oxygen than in the presence of oxygen (data not shown): with 10 μM Cu^{2+}, decomposition of the C-1 alkyl glycoside chloramides was

(38) Fossey, J.; Lefort, D.; Sobra, J. *Free Radicals in Organic Chemistry*; Wiley: Chichester, 1995.
(39) Hawkins, C. L.; Davies, M. J. *J. Chem. Soc., Perkin Trans. 2* **1998**, 1937−1945.
(40) Thomas, E. L.; Grisham, M. B.; Jefferson, M. M. *Methods Enzymol.* **1986**, *132*, 569−585.
(41) Hazell, L. J.; Davies, M. J.; Stocker, R. *Biochem. J.* **1999**, *339*, 489−495.

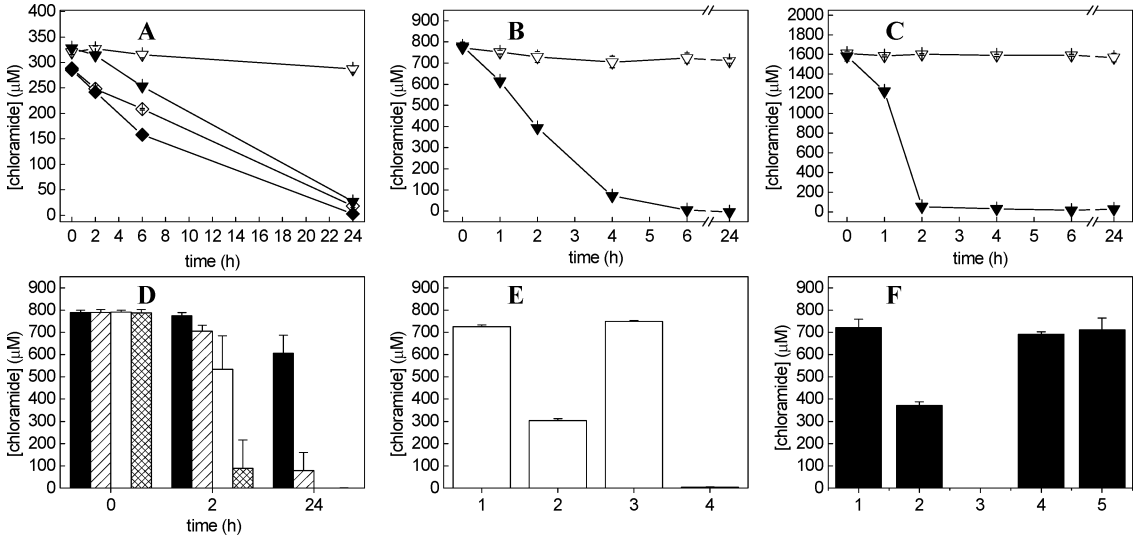

Figure 1. Time course of decomposition of monomer and polymer chloramides. (A) *N*-Acetyl glucosamine (*diamonds*) and β-methyl glycoside chloramides (*triangles*) under aerobic conditions at 37 °C, pH 7.4, in the absence (*open symbols*) and presence (*closed symbols*) of 10 μM Cu^{2+}. (B) Chondroitin-4-sulfate chloramides incubated under aerobic conditions at 37 °C in the absence (*open symbols*) and presence (*closed symbols*) of 500 nM Cu^{2+} at pH 7.4. (C) As (B), except with hyaluronan chloramides. (D) Chondroitin-4-sulfate chloramides incubated under aerobic conditions at 37 °C, pH 7.4 in the absence of Cu^{2+} (*closed bars*), or with 10 nM (*slashed bars*), 100 nM (*open bars*), or 1000 nM (*hatched bars*) Cu^{2+}. (E) Chondroitin-4-sulfate chloramides incubated with 0 (lanes 1, 3) or 500 nM (lanes 2, 4) Cu^{2+} at 37 °C for 2 h under aerobic (lanes 1, 2) or anoxic conditions (lanes 3, 4). (F) Chondroitin-4-sulfate chloramides incubated under aerobic conditions at 37 °C for 2 h with 0 (lane 1) or 500 nM (lanes 2−5) Cu^{2+} and excess methionine (lane 3), 0.05 mg/mL SOD (lane 4) or 500 nM EDTA (lane 5). Data points are the mean ± SD of six determinations from two separate experiments (A−C) or the mean ± SD of at least three separate experiments (D−F).

incomplete within 26 h under aerobic conditions, but complete under anoxic conditions.

Incubation of the polymer chloramides with Cu^{2+} (454 μM) at 21 °C and pH 7.4 under anoxic conditions induced significant decomposition within 20 min, consistent with the data above. Fe^{3+} (364 μM) or Fe^{3+}-EDTA (364 μM) did not induce significant decomposition under identical conditions. The corresponding low-valent species at the same concentrations [Cu^{+} (generated by reaction of Cu^{2+} (454 μM) with Ti^{3+} (364 μM)[10,31]), Ti^{3+} alone (as a control for the Cu^{+}-generating system), Fe^{2+}, Fe^{2+}-EDTA] decomposed these materials rapidly, although the extent of loss varied with the metal ion. Cu^{+} and Ti^{3+} induced the most extensive decomposition, and in these cases (but not Fe^{2+} or Fe^{2+}-EDTA) the concentration of chloramides lost exceeded that of the metal ions added, consistent with the occurrence of chain reactions. Fe^{2+}-EDTA induced less decomposition than Fe^{2+}. With the chloramides of *N*-acetyl glucosamine, di-*N*-acetyl chitobiose, and the C-1 alkyl glycosides, inclusion of Cu^{+} (or Ti^{3+}, as above) under anoxic conditions also resulted in rapid chloramide decomposition. Under aerobic conditions, the extent of loss of the chloramides induced by these metal ions was substantially less than that detected under anoxic conditions. This effect is likely to be due to competing autooxidation reactions.

Thermal decomposition of *N*-acetyl glucosamine chloramide (5.7 mM) at 21 °C or 37 °C at pH 7.4 in the presence of the spin trap MNP (18.2 mM) gave weak EPR signals. Analogous experiments with the β-isopropyl glycoside chloramide or the polymer chloramides, gave either no detectable signals or very weak signals (data not shown) as expected from the slow spontaneous decomposition of these materials (cf. Figure 1). In contrast, decomposition of preformed chloramides (0.23−1.1 mM) by Cu^{+} (0.33 mM, generated as above) at 21 °C at pH 7.4 in the presence of spin traps (MNP 17 mM or DMPO 83 mM) under anoxic conditions gave intense EPR spectra in all cases (Figures 2 and 3). With *N*-acetyl glucosamine chloramide and the β-isopropyl glycoside chloramide, these signals were identical to, but more intense than, those detected in the absence of added metal ions. No substrate-derived radicals were detected when (i) the parent compounds were exposed to Cu^{+} under the same conditions, (ii) the chloramides were quenched by reaction with excess methionine[40] before addition of Cu^{+}, and (iii) the spin trap was omitted from the reaction mixture. With each substrate, the maximum signal intensity was observed in the initial spectra acquired, consistent with the rapid reaction of Cu^{+} with the chloramides. Over a period of up to 60 min, a slow species-dependent decrease in the total radical adduct concentration was observed. With the alkyl glycosides and MNP, identical but less intense spectra were also detected under aerobic conditions. All subsequent experiments described below were performed under anoxic conditions using Cu^{+} to promote chloramide decomposition unless stated otherwise.

The spectral data for all the species detected, together with assignments, are given in Tables 1 and 2 (Supporting Information). The latter are based on observed splitting patterns and comparison of the hyperfine coupling constants with data for related species (refs 39,42 see also: http://EPR.niehs.nih.gov/stdb). The measured hyperfine coupling constants were confirmed by computer simulation. With each substrate, and both spin traps, the major species detected by EPR are assigned to adducts of carbon-centered radicals arising from the occurrence of rapid rearrangement of an initial amidyl radical (cf. data for related species[39]).

With *N*-acetyl glucosamine chloramide, signals assigned to multiple isomeric adducts of a C-2-derived carbon-centered radical were detected whose ratios changed markedly with time, though the total radical adduct concentration remained relatively constant (as assessed by double integration of the EPR signals)

(42) Buettner, G. R. *Free Radical Biol. Med.* **1987**, *3*, 259−303.

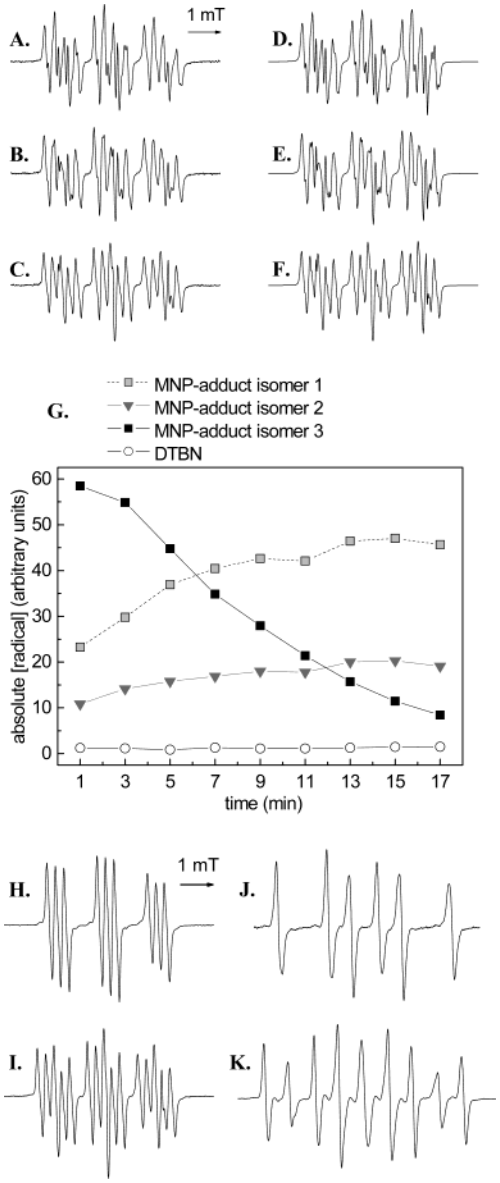

Figure 2. EPR spectra of spin adducts detected on decomposition of *N*-acetyl glucosamine chloramides in the presence of Cu^{+}. *N*-Acetyl glucosamine and *N*-acetyl [2-^{13}C]-glucosamine chloramides (ca. 230 μM) were incubated with Cu^{+} (327 μM) at ca. 21 °C under anoxic conditions in the presence of MNP (17 mM; (A−C, H, I)) or DMPO (83 mM; (J, K)). *N*-Acetyl [2-^{13}C]-glucosamine chloramides and Cu^{+} after 1 min (A), 7 min (B), or 17 min (C). (D−F) Computer simulations of the spectra in (A−C) respectively using the following components: three isomeric MNP-adducts of the *N*-acetyl glucosamine C-2 carbon-centered radical [a(N) = 1.56 mT, a(β-H) = 0.10 mT, a(β-N) = 0.26 mT; a(N) = 1.56 mT, a(β-N) = 0.26 mT; a(N) = 1.54 mT, a(β-H) = 0.09 mT, a(β-N) = 0.30 mT] and the spin trap degradation product di-*tert*-butylnitroxide [a(N) = 1.71 mT]. (G) Absolute concentrations of these radicals over time. (H, I) As (A−C), except with unlabeled *N*-acetyl glucosamine chloramide (H) or *N*-acetyl [2-^{13}C]-glucosamine chloramides (I), 19 min after addition of Cu^{+}. Parameters of adducts in I, as (A−C) except with an additional coupling a(^{13}C) = 0.48 mT, a(^{13}C) = 0.48 mT, a(^{13}C) = 0.30 mT respectively for the three isomeric adducts. (J) As (H) except with DMPO and 19 min after addition of Cu^{+} [a(N) = 1.56 mT, a(β-H) = 2.29 mT; a(N) = 1.55 mT, a(β-H) = 2.12 mT]. (K) As (I) except with DMPO (83 mM) and 19 min after addition of Cu^{+}. Parameters of adducts as in (I), except with an additional coupling a(^{13}C) = 0.74 mT and a(^{13}C) = 0.82 mT, respectively. All spectra were obtained using identical spectrometer conditions except for the magnetic field scan (MNP: 6.5 mT, DMPO 8−10 mT).

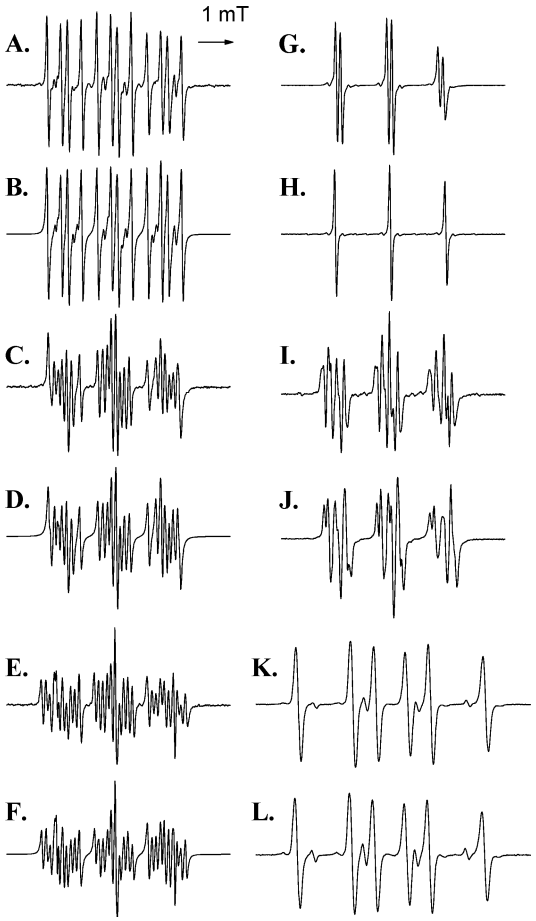

Figure 3. EPR spectra of spin adducts detected on decomposition of *N*-acetyl glucosamine alkyl glycoside chloramides in the presence of Cu^{+} and MNP (A−J) or DMPO (K, L). Chloramides (ca. 250−1350 μM) were exposed to Cu^{+} (327 μM) at 21 °C, pH 7.4, and EPR spectra were acquired 2 min after addition of Cu^{+} unless otherwise stated. (A) α-Methyl glycoside chloramide. (B) Simulation of (A) using two components assigned to the C-2 carbon-centered radical adduct [a(N) = 1.54 mT, a(β-H) = 0.12 mT, a(β-N) = 0.26 mT] and an adduct of a radical from the α-methyl group ($^{\bullet}$CH$_2$O-sugar) [a(N) = 1.46 mT, a(β-H) = 0.60 mT, a(β-H) = 0.40 mT]. (C) β-Methyl glycoside chloramide. (D) Simulation of (C) using two components assigned to the C-2 carbon-centered radical adduct [a(N) = 1.54 mT, a(β-H) = 0.13 mT, a(β-N) = 0.25 mT] and an adduct of a radical from the β-methyl group ($^{\bullet}$CH$_2$O-sugar) [a(N) = 1.45 mT, a(β-H) = 0.53 mT, a(β-H) = 0.39 mT]. (E) [2-^{13}C]-β-methyl glycoside chloramide. (F) Simulation of (E) using data from (C) with an additional coupling a(^{13}C) = 0.47 mT. (G) β-Ethyl glycoside chloramide; signals assigned to two isomeric adducts of $^{\bullet}$CH(CH$_3$)O-sugar radicals [a(N) = 1.48 mT, a(β-H) = 0.14 mT; a(N) = 1.51 mT, a(β-H) = 0.13 mT] plus the C-2 carbon-centered radical adduct [a(N) = 1.54 mT, a(β-H) = 0.12 mT, a(β-N) = 0.25 mT]. (H) β-Isopropyl glycoside chloramide; signals assigned to two isomeric adducts of the $^{\bullet}$C(CH$_3$)$_2$O-sugar radical [a(N) = 1.60 mT; a(N) = 1.62 mT] plus a species assigned to a $^{\bullet}$CH$_2$CH(CH$_3$)O-sugar radical adduct [a(N) = 1.72 mT, a(2H) = 0.71 mT]. (I) β-*tert*-Butyl glycoside chloramide at pH of 8.5 (identical but weaker signals were observed at pH 7.4); signals assigned to two isomeric adducts of the C-2 carbon-centered radical [a(N) = 1.57 mT, a(β-H) = 0.13 mT, a(N) = 0.23 mT; a(N) = 1.56 mT, a(β-H) = 0.19 mT, a(N) = 0.23 mT] and an unknown adduct species with [a(N) = 1.60 mT]. (J) 2-Acetamido-2-deoxy-3-*O*-methyl-D-glucopyranoside chloramide with spectrum acquired 19 min after addition of Cu^{+}. Signals assigned to three isomeric adducts of the C-2 carbon-centered radical [a(N) = 1.56 mT, a(β-H) = 0.08 mT, a(N) = 0.24 mT; a(N) = 1.56 mT, a(N) = 0.24 mT; a(N) = 1.54 mT, a(β-H) = 0.11 mT, a(N) = 0.31 mT]. (K) β-Methyl glycoside chloramide. (L) [2-^{13}C]-β-Methyl glycoside chloramide. Signals in (K) and (L) assigned to two isomeric adducts of radicals derived from the β-methyl group [a(N) = 1.62 mT, a(β-H) = 2.27 mT; a(N) = 1.56 mT, a(β-H) = 2.25 mT]. All spectra were recorded using identical spectrometer conditions except for the magnetic field scan width (MNP 6.5 mT, DMPO 8.0 mT).

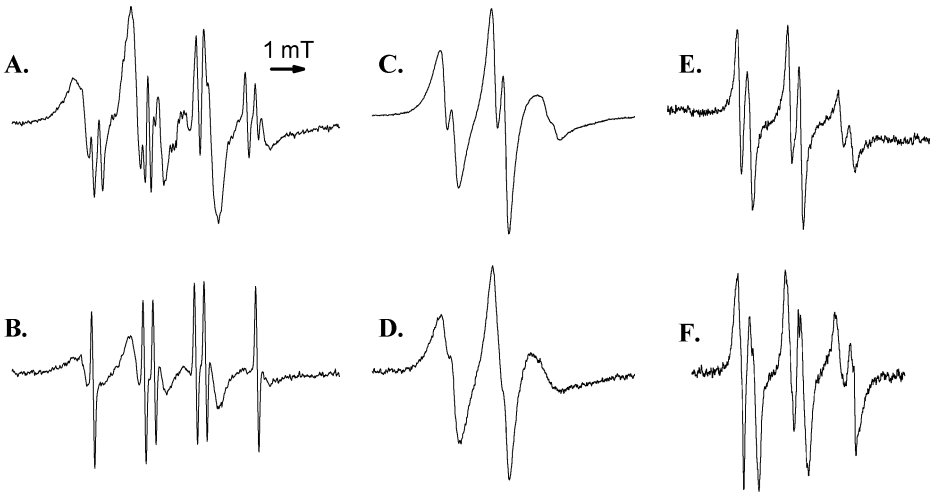

Figure 4. EPR spectra of spin adducts detected on decomposition of glycosaminoglycan and hexa-*N*-acteyl chitohexaose chloramides in the presence of DMPO (A,B) or MNP (C−F). (A) Hyaluronan chloramides (1.3 mM) incubated with Cu^+ (327 μM) at 21 °C, pH 7.4, in the presence of DMPO (83 mM) with the spectrum acquired 2 min after addition of Cu^+. (B) As (A) except with chondroitin-4-sulfate chloramides (570 μM). (C, D) As (A, B) respectively, except with MNP (17 mM) as the spin trap, and with low-molecular-mass species removed by size-exclusion (PD10) chromatography before analysis. (E) As (C) except after incubation of the high-molecular-mass, hyaluronan-derived, adducts with testicular hyaluronidase (6500 units/mL, 37 °C, pH 7.4, 2 h) and the resulting low-molecular-mass fraction obtained by size-exclusion (PD10) chromatography examined by EPR. (F) As (A) except with hexa-*N*-acetyl chitohexaose chloramides (260 μM) with the spectrum acquired 1 min after addition of Cu^+. All spectra were recorded using identical spectrometer conditions except for the magnetic field scan width (MNP 6.5−8.0 mT, DMPO 10.0 mT).

(Figure 2, A−G). The assignment of these signals to adducts of C-2-derived species was confirmed using [2-^{13}C] labeling, which gave the expected additional ^{13}C couplings with both spin traps (Figure 2, H−K). With the C-1 (α- and β-) methyl glycosides, and MNP as the spin trap, features assigned to both the C-2 carbon-centered radical adduct (confirmed by [2-^{13}C] labeling) and an adduct of a radical with partial structure $^{\bullet}CH_2R$ with inequivalent methylene hydrogens were detected (Figure 3, A−F); the second species predominated with the α-isomer (Figure 3, A vs C). Adducts of radicals with partial structure $^{\bullet}CHRR'$ were detected with the β-ethyl glycoside (Figure 3G), and adducts of two species with partial structures $^{\bullet}CRR'R''$ (major) and $^{\bullet}CH_2R'$ (minor) were detected with the β-isopropyl glycoside (Figure 3H); the latter signal is assigned to an adduct of a radical arising from hydrogen abstraction from the isopropyl methyl groups. The relative yield of the C-2 carbon-centered radical adduct detected with the parent alkyl glycoside chloramide decreased along the series β-methyl > β-ethyl > β-isopropyl, with this species being undetectable in the last case. With the β-*tert*-butyl glycoside chloramide, the C-2 carbon-centered radical adduct was the major species detected (Figure 3I). In contrast to the above behavior, with 2-acetamido-2-deoxy-3-*O*-methyl glucopyranoside chloramide, where the methyl glycoside is present at the C-3 position rather than C-1, only the C-2 carbon-centered radical was detected, suggesting that hydrogen abstraction from the C-3 methyl group does not occur readily. Confirmation that the adducts detected with the β-methyl isomer arise from trapping of a $^{\bullet}CH_2O$-sugar radical derived from the glycosidic methyl group was obtained from experiments using the [2-^{13}C]-labeled species—the radical adducts detected using DMPO as the trap were unaffected by this isotopic substitution (Figure 3, K,L).

With each substrate, the addition of methanol or glucose (up to 1.3 M) did not affect the spectra observed (data not shown). Furthermore, with *N*-acetyl [2-^{13}C]-glucosamine chloramide, and a 5-fold excess of unlabeled *N*-acetyl glucosamine, only adducts from the ^{13}C-labeled compound were observed (data not shown). These data are consistent with intra-, but not inter-, molecular hydrogen atom abstraction reactions induced by a primary amidyl radical giving rise to the species detected.

N-Acetyl allolactosamine chloramide gave only signals assigned to adducts of a C-2 carbon-centered radical on the *N*-acetyl glucosamine ring (three MNP adduct isomers: [a(N) = 1.54 mT, a(β-H) = 0.10 mT, a(N) = 0.26 mT; a(N) = 1.54 mT, a(N) = 0.26 mT; a(N) = 1.53 mT, a(β-H) = 0.13 mT, a(N) = 0.31 mT] and two DMPO isomers [a(N) = 1.57 mT, a(β-H) = 2.25 mT; a(N) = 1.50 mT, a(β-H) = 2.24 mT]), whereas with the chloramides of di-*N*-acetyl chitobiose, tri-*N*-acetyl chitotriose, and hexa-*N*-acetyl chitohexaose (chitin oligosaccharides) signals assigned to adducts of C-2 carbon-centered radicals located on the terminal (reducing) *N*-acetyl glucosamine rings (three MNP adduct isomers [a(N) = 1.55 mT, a(β-H) = 0.10 mT, a(N) = 0.24 mT; a(N) = 1.55 mT, a(N) = 0.24 mT; a(N) = 1.52 mT, a(β-H) = 0.08 mT, a(N) = 0.21 mT]), and further signals assigned to adducts of C-4 carbon-centered radicals (Scheme 3; MNP adduct [a(N) = 1.52 mT]) and a short-lived adducts of radicals with partial structure $^{\bullet}CHRR'$ were detected (MNP adduct [a(N) = 1.50 mT, a(β-H) = 0.36 mT]). With hexa-*N*-acetyl chitohexaose, the major species detected was the $^{\bullet}CHRR'$ adduct (Figure 4F).

With the polymer chloramides, reaction with Cu^+ (as above) in the presence of DMPO (102 mM) gave both broad polymer-derived radical adduct signals [a(N) ca. 1.5−1.7 mT, a(β-H) ca. 2.2−2.4 mT] and features assigned to the $CO_2^{\bullet-}$ adduct ([a(N) = 1.57 mT, a(β-H) = 1.86 mT] (Figure 4, A,B). The broad signals have been assigned to adducts of polymer-derived carbon-centered radicals, which coeluted with the parent polymer on size-exclusion (PD10) chromatography, consistent with these being high-molecular-mass species. With MNP (20.4 mM) as the trap, intense, anisotropic EPR signals consistent with assignment to one or more slowly tumbling, polymer-derived radical adducts were detected (Figure 4, C,D). Analogous, although less intense, signals were detected using Fe^{2+}, Fe^{2+}-EDTA, or Ti^{3+} in place of Cu^+ (data not shown). No

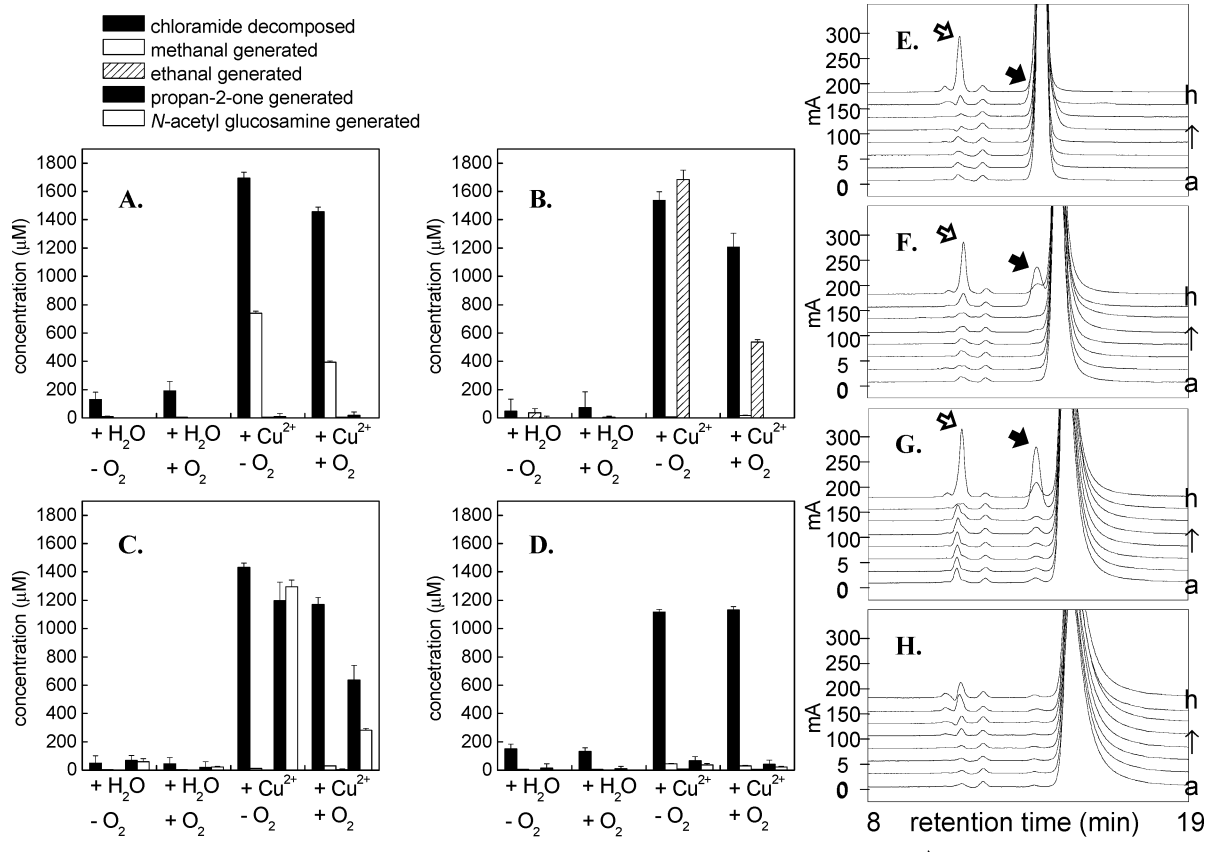

Figure 5. Quantification of fragmentation products formed on decomposition of *N*-acetyl glucosamine alkyl glycoside chloramide derivatives. (A−D) Alkyl glycoside chloramides (ca. 1100−1500 μM) were incubated under the indicated conditions (absence or presence of 10 μM Cu^{2+}; anoxic or aerobic conditions) at 37 °C for 26 h. Chloramide concentrations were determined prior to and post incubation, and chloramide loss was quantified using the TNB assay. Formation of methanal, ethanal, and propan-2-one was quantified by HPLC as their 2,4-dinitrophenyl hydrazones. (A) β-Methyl glycoside chloramide (1.69 mM). (B) β-Ethyl glycoside chloramide (1.56 mM). (C) β-Isopropyl glycoside chloramide (1.44 mM). (D) β-*tert*-Butyl glycoside chloramide (1.11 mM). (E−H) The reaction mixtures from (A−D), respectively, analyzed after incubation (but without derivatization) by use of gel permeation/ligand-exchange chromatography with photodiode array detection (chromatograms obtained at 200 nm are displayed). The elution position of authentic *N*-acetyl glucosamine (13.7 min) is indicated by black arrows; an unidentified amide product, believed to be *N*-acetyl glucosaminic acid (11.2 min) is indicated by gray arrows; for β-methyl glycoside chloramide (E) quantification of *N*-acetyl glucosamine was prevented due to its coelution with the parent glycoside (off-scale peak), and for β-ethyl glycoside chloramide (F) quantification was not attempted due to partial interference from the parent glycoside (off-scale peak). HPLC reaction traces for (E−H): trace (a) parent amide in absence of Cu^{2+} under anoxic conditions, (b) parent amide in absence of Cu^{2+} under aerobic conditions, (c) parent amide in absence of Cu^{2+} under anoxic conditions, (d) parent amide in the presence of Cu^{2+} under aerobic conditions, (e) chloramide in absence of Cu^{2+} under anoxic conditions, (f) chloramide in absence of Cu^{2+} under aerobic conditions, (g) chloramide in absence of Cu^{2+} under anoxic conditions, (h) chloramide in the presence of Cu^{2+} under aerobic conditions. All data points are the mean ± SD of six determinations from two independent experiments.

polymer-derived adduct species were detected using MNP as the spin trap in experiments with the parent polymer when the chloramides were quenched with excess methionine prior to reaction with Cu^{+} or when the chloramides were incubated with Fe^{3+}, Fe^{3+}-EDTA, Cu^{2+} or Ti^{4+}.

Digestion of the preformed, polymer-derived, MNP adducts with testicular hyaluronidase (6500 units/mL, 37 °C, pH 7.4, 2 h) resulted in sharper EPR signals consistent with the release of mobile, low-molecular-mass radical adducts from both polymers (Figure 4E). The predominant signal detected with both species has been assigned to adducts of radicals with the partial structure $^{\bullet}$CHRR′ [a(N) = 1.55 mT, a(β-H) = 0.31 mT]) analogous to those observed with the chitin oligosaccharides (e.g. from hexa-*N*-acetyl chitohexaose; Figure 4F). Additional signals assigned to adducts of C-4 tertiary carbon-centered radicals [a(N) = 1.53 mT] were also detected.

Cu^{2+}-induced decomposition of the β-methyl, β-ethyl and β-isopropyl glycoside chloramides (10 μM Cu^{2+}, pH 7.4, 37 °C, 26 h) under both aerobic and anoxic conditions, gave high yields of methanal, ethanal and propan-2-one respectively (Figure 5, A−D). In each case, lower yields were detected in the presence of O_2. Identical products were detected, at comparable concentrations, using Cu^{+} (364 μM, as above) or Ti^{3+} (364 μM) as the catalysts to decompose the chloramides (21 °C, 20 min) under anoxic conditions (results not shown). Similar experiments with Cu^{+} or Ti^{3+} under aerobic conditions, where chloramide decomposition is limited (see above), gave low yields of carbonyl products. Reaction of Cu^{2+} (pH 7.4, 37 °C, 26 h) or Cu^{+} (21 °C, 20 min), at identical concentrations, with the parent amides did not yield significant quantities of these products (results not shown). Incubation of the β-methyl, β-ethyl and β-isopropyl glycoside chloramides in the absence of added agents, where chloramide decomposition is limited, gave correspondingly lower concentrations of the carbonyl products.

Analysis, by HPLC with UV detection, of the above reaction mixtures, resulted in the detection of a product with retention time (13.7 min) and UV−visible spectrum identical to those of

authentic *N*-acetyl glucosamine under both aerobic and anoxic conditions (Figure 5, E−G). A further product, which eluted at 11.2 min, was also detected. This material had a UV−visible spectrum that was essentially identical to that of *N*-acetyl glucosamine and thus is believed to possess an amide function. The detection of both products required the presence of all components of the reactions mixtures, and these materials were not detected with the parent alkyl glycosides. The yield of *N*-acetyl glucosamine was decreased and the yield of the unidentified product increased under aerobic conditions when compared to anoxic experiments (Figure 5, C,E−G). Neither product was detected in significant yield upon decomposition of the *β-tert*-butyl glycoside chloramide under analogous conditions (Figure 5H).

Decomposition of di-*N*-acetyl chitobiose chloramides in the presence of Cu^{2+} (10 μM, pH 7.4, 37 °C, 26 h) also gave *N*-acetyl glucosamine, with higher yields detected under anoxic conditions compared to those under aerobic conditions. The unidentified product with retention time of 11.2 min was detected under both aerobic and anoxic conditions, with higher yields detected under anoxic conditions. Decomposition induced by Cu^{+} (364 μM, as above) or Ti^{3+} (364 μM) (21 °C, 20 min) under anoxic conditions also gave *N*-acetyl glucosamine in high yield; this material was not detected under aerobic conditions (results not shown), consistent with the limited decomposition induced by these metal ions under the latter conditions.

Incubation of hyaluronan and chondroitin-4-sulfate in the absence of added metal ions at 4, 22, 37, or 50 °C and pH 7.4 over 24 h did not give rise to significant polymer fragmentation as assessed by PAGE with Alcian Blue staining and densitometric analysis. Incubation of the corresponding chloramides under the same conditions resulted in polymer fragmentation at 50 °C, but not lower temperatures, consistent with the stability of these chloramides.

Inclusion of Cu^{2+} (10 nM to 100 μM) in such reactions at 37 °C and pH 7.4 resulted in a time-, concentration-, and O_2-dependent fragmentation of the polymer as assessed by PAGE (Figure 6, Panels A,B) and gel permeation chromatography (data not shown). Upon complete decomposition of the chloramides as assessed by TNB assay, no further polymer fragmentation was observed. The maximum extent of fragmentation detected in the presence of Cu^{2+} was similar under anoxic and aerobic conditions as assessed by both PAGE or gel permeation chromatography (data not shown). With hyaluronan chloramides, analysis by gel permeation chromatography also resulted in the detection of a product with retention time and UV−visible spectrum identical to those of authentic *N*-acetyl glucosamine (data not shown).

With 500 nM Cu^{2+} at 37 °C and pH 7.4 under aerobic conditions, polymer fragmentation reached maximal levels within 24 h. Under anoxic conditions decomposition was more rapid, with fragmentation reaching maximal levels within 2 h (Figure 6, Panels C,D). No fragmentation was observed when the parent polymers were exposed to identical reaction conditions or when the chloramides were quenched by reaction with excess methionine before addition of the metal ion. Inclusion of EDTA (500 nM), SOD (196 units/mL; 0.05 mg/mL), and BSA (0.05 mg/mL) under aerobic conditions decreased the extent of polymer fragmentation (Figure 6, Panels E,F). The protection afforded by SOD was unaffected by the exclusion of O_2, suggestive of a nonspecific effect of the protein.

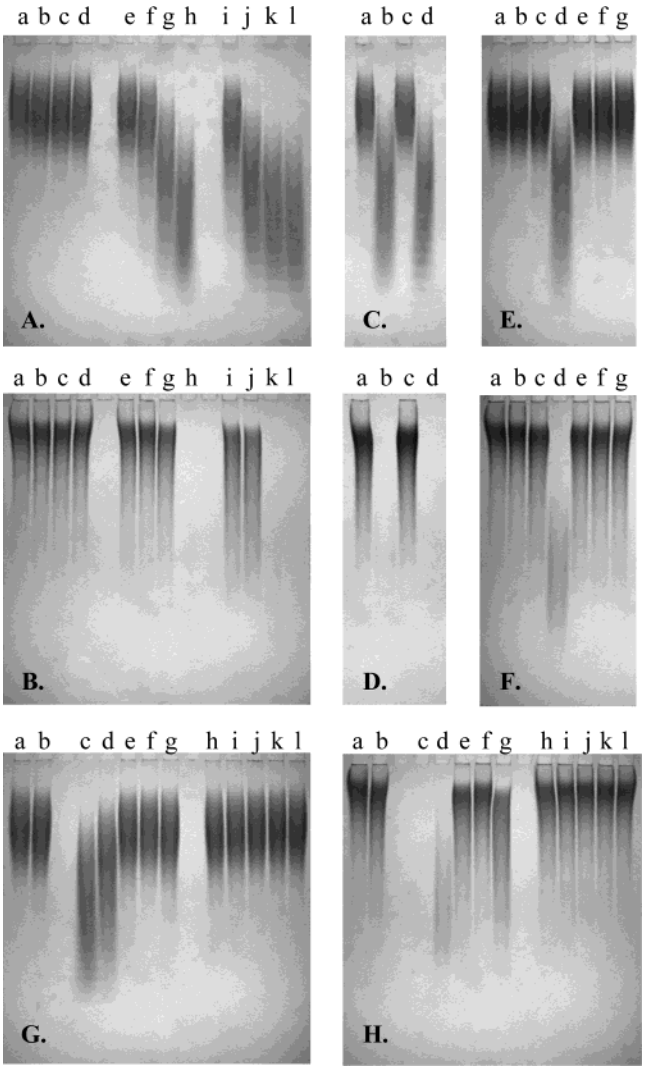

Figure 6. Analysis of structural integrity of glycoaminoglycans on decomposition of chloramides in the presence and absence of Cu^{2+} under aerobic and anoxic conditions. Chloramides were generated as described in the text and subsequently decomposed as outlined below. Samples were subsequently analyzed using 20% polyacrylamide gels stained with Alcian Blue. (A) Chondroitin-4-sulfate chloramides incubated with in the absence (lanes a, e, i) or presence of 10 nM (lanes b, f, j), 100 nM (lanes c, g, k) or 1000 nM (lanes d, h, l) Cu^{2+} under aerobic conditions at 37 °C for 0 (lanes a−d), 2 (lanes e−h), or 24 h ((lanes i−l). (B) As (A) except with hyaluronan chloramides. (C) Chondroitin-4-sulfate chloramides incubated with 0 (lanes a, c) or 500 nM (lanes b, d) Cu^{2+} under aerobic (lanes a, b) or anoxic (lanes c, d) conditions at 37 °C for 2 h. (D) As (C) except with hyaluronan chloramides. (E) Chondroitin-4-sulfate (lane a, b) or chondroitin-4-sulfate chloramides (lanes c−g) incubated with 0 (lane a, c) or 500 nM (lanes b, d−g) Cu^{2+} under aerobic conditions at 37 °C for 2 h in the absence of other added agents, or in the presence of lane e − excess methionine, lane f − 0.05 mg/mL SOD, lane g − 500 nM EDTA. (F) As (E), except with hyaluronan and hyaluronan chloramides. (G) Chondroitin-4-sulfate chloramides (650 μM, lanes b−g) incubated with water (lane b) Cu^{+} (lane c) Ti^{3+} (lane d), Cu^{2+} (lane e), Ti^{4+} (lane f), or Cu^{2+} plus Ti^{4+} (lane g) (all metal ions 364 μM, except Cu^{2+}, 454 μM) for 20 min under anoxic conditions at 21 °C. Chondroitin-4-sulfate (lanes a,h−l) incubated with water (lane a) Cu^{+} (lane h) Ti^{3+} (lane i), Cu^{2+} (lane j), Ti^{4+} (lane k), or Cu^{2+} plus Ti^{4+} (lane l) (all metal ions 364 μM, except Cu^{2+}, 454 μM) for 20 min under anoxic conditions at 21 °C. (H) As (G), except with hylauronan chloramides (1.55 mM) and hyaluronan. All gels are representative analyses of three or more, separate experiments. The absence of staining in some of the lanes from the hyaluronan experiments is due to the presence of very low-molecular-mass fragments that do not readily bind Alcian Blue.

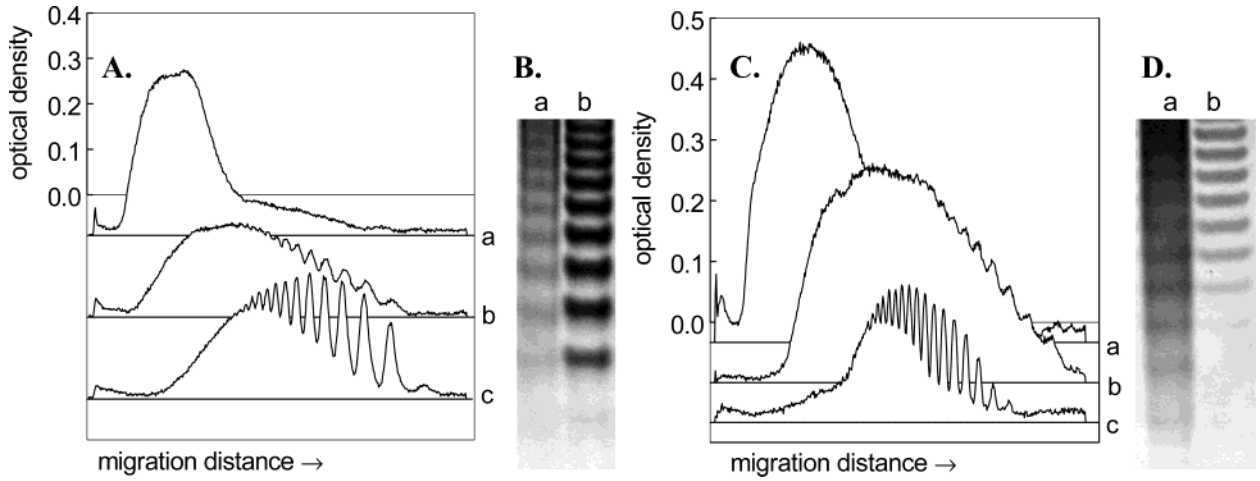

Figure 7. Decomposition of glycosaminoglycan chloramides by metal ions gives rise to specific fragments as evidence by PAGE. (A) Densitometric analysis of chondroitin sulfate samples separated on 30% polyacrylamide gels and subsequently stained with Alcian Blue. Trace a: chondroitin-4-sulfate chloramides (650 μM) incubated under anoxic conditions at 21 °C for 20 min in the absence (trace a) or presence of Cu^{+} (364 μM, trace b). Banding similar to that shown in trace b was detected on incubation of identical chloramide samples with 10 μM Cu^{2+} under anoxic conditions at 37 °C for 2 h. Trace c, chondroitin-4-sulfate enzymatically digested with testicular hyaluronidase for 1 h (see Experimental Section). (B) Expanded view of gel in (A): lane a as for trace b; lane b, as for trace c. (C) As (A), except with hyaluronan chloramides (900 μM) and incubation at 21 °C for 20 min, with 30% polyacrylamide gels stained using a combined Alcian Blue and silver staining method (see Experimental Section). Trace c, hyaluronan digested with testicular hyaluronidase for 2.5 h (see Experimental Section). (D) Expanded view of gel analyzed in (C): lane a, as for trace b, lane b, as for trace c.

Fragmentation was also detected on incubation of both polymer chloramides with Cu^{+} (generated as above), Ti^{3+}, Fe^{2+}, or Fe^{2+}-EDTA, (all 364 μM) for 20 min at pH 7.4 and 21 °C under anoxic conditions, but not with Fe^{3+}, Fe^{3+}-EDTA, Ti^{4+}, or EDTA alone at identical concentrations (Figure 6, Panels G,H). Fragmentation was also observed, to a limited extent in the presence of Cu^{2+} (454 μM) (Figure 6, Panels G,H). Cu^{+} and Ti^{3+} induced the greatest extent of fragmentation, and Fe^{2+} was more effective than Fe^{2+}-EDTA (data not shown). These data correlate well with the extents of chloramide decomposition induced by these metal ions (data not shown). The fragmentation induced by Cu^{+} and Ti^{3+} was less marked in the absence of O_2 than in its presence (data not shown), consistent with the lower extent of chloramide decomposition under the latter conditions. In the presence of O_2 (but not in its absence), depolymerization was observed to occur to a small extent upon exposure of the parent polymers to Cu^{+} and Ti^{3+} (data not shown); this is attributed to the production of $HO^{\bullet}$ upon autooxidation of these metal ions.

High-resolution PAGE analysis of Cu^{2+}- and Cu^{+}-treated chondroitin-4-sulfate and hyaluronan chloramides gave regular banding on the gels, consistent with the formation of discrete low-molecular-mass oligosaccharides. These fragments were compared with those obtained from partial enzymatic digestion of the parent polymers by testicular hyaluronidase (Figure 7) which generates a homologous series, differing only in the number of disaccharide repeat units, as a result of hydrolytic cleavage of the polymers at the *N*-acetyl-glycosamine β-(1→4) glycosidic bonds.[43] This comparison reveals that the chloramide-dependent polymer fragmentation occurs via selective cleavage at disaccharide intervals, resulting in equidistant spacing of the bands in the two "ladders". Differences in absolute extent of migration of the observed bands suggest that they have different overall structures. This banding was more distinct in the absence of O_2, consistent with the occurrence of competing reactions under aerobic conditions.

Discussion and Conclusions

Reaction of HOCl with amide-containing mono-, oligo-, and polysaccharides gives chloramides as assessed by both UV−visible spectroscopy and assay using TNB. The kinetics of these reactions varies with the structure of the substrate, with the rate decreasing with increasing steric bulk at the glycosidic position in accord with previous studies.[11] Myeloperoxidase in the presence of H_2O_2 and physiological levels of chloride ion also generates glycosaminoglycan chloramides, suggesting that such species will be generated in vivo in locations (such as inflammatory foci) where this enzyme is released from activated monocytes and macrophages.[44−46] The highly basic nature of this protein results in electrostatic binding of this enzyme to polyanionic extracellular matrix glycosaminoglycans.[14,15] Such an association may localize oxidation to such sites and result in selective damage to these components; evidence has recently been presented for this phenomenon.[32]

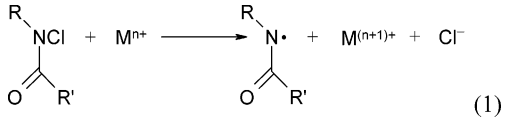

(1)

The rate of chloramide decomposition depends on the chloramide structure, reaction temperature, and the presence of redox-active metal ions. Unlike many amino acid-derived chloramines,[39] the chloramides formed on these substrates are long-lived at 37 °C in the absence of other agents. The stimulation of chloramide decomposition by metal ions such as Cu^{+} and Fe^{2+} has been ascribed to one-electron reduction

(43) Cowman, M. K.; Slahetka, M. F.; Hittner, D. M.; Kim, J.; Forino, M.; Gadelrab, G. *Biochem. J.* **1984**, *221*, 707−716.
(44) Daugherty, A.; Dunn, J. L.; Rateri, D. L.; Heinecke, J. W. *J. Clin. Invest.* **1994**, *94*, 437−444.
(45) Hazell, L. J.; Baernthaler, G.; Stocker, R. *Free Radical Biol. Med.* **2001**, *31*, 1254−1262.
(46) Sugiyama, S.; Okada, Y.; Sukhova, G. K.; Virmani, R.; Heinecke, J. W.; Libby, P. *Am. J. Pathol.* **2001**, *158*, 879−891.

of the chloramide with the formation of an amidyl radical and Cl^- (eq 1).[11,39] With most of the chloramides examined, the concentration of chloramides lost on exposure to Cu^+ in the absence of O_2, exceeded that expected from a stoichiometric reaction, consistent with the occurrence of chain reactions, and recycling of the metal ions. This is believed to involve regeneration of Cu^+ from Cu^{2+} by substrate-derived radicals, and/or reduction of the metal ion by reducing sugars. Support for the occurrence of the latter process arises from the observation of a slow rate of chloramide decomposition in the presence of Cu^{2+}, although oxidation of radicals by Cu^{2+}, with the regeneration of Cu^+, may also occur (cf. data from other systems[47]). Chloramide reduction by Fe^{2+} or Fe^{2+}-EDTA has been shown to be less facile than that induced by Cu^+. The reason for the variation in the rate and extent of chloramide decomposition induced by these metal ions tested is likely to be multifactorial and to encompass both the redox potentials of these ions and electronic and steric interactions with the substrate (particularly for polysaccharides) and the surrounding ligands. The lower extent of chloramide reduction induced by Cu^+ in the presence of O_2 is ascribed to competing autooxidation of the metal ions. The protective effect of EDTA against Cu^{2+}-mediated chloramide decomposition is consistent with the formation of a stable, negatively charged, low-reduction-potential complex with EDTA.[48] The ability of both BSA and SOD to inhibit these reactions is believed to be due to the metal ion binding by these proteins to give inactive complexes.[49]

Evidence has been presented for radical formation during chloramide decomposition, with high yields of these intermediates detected in the presence of those metal ions which induced rapid, and extensive, chloramide decomposition. The primary radicals generated as a result of such reactions are believed to be amidyl radicals (eq 1); analogous species have been detected directly (by use of EPR spectroscopy and spin trapping with DMPO) with other chloramides where subsequent rearrangement and fragmentation reactions are slow (e.g. from *N-tert*-butyl acetamide and succinimide[50]). No direct evidence has been obtained for the formation of amidyl radicals in the current study, even with near molar concentrations of spin trap; this is ascribed to the occurrence of rapid intramolecular radical rearrangement reactions. This interpretation is consistent with the observation that molar concentrations of alternative targets, such as glucose and methanol also do not compete effectively with the postulated intramolecular rearrangements under the conditions employed.

With *N*-acetyl glucosamine, the spin adducts detected on chloramide decomposition have been assigned to multiple isomeric adducts of the C-2 carbon-centered radical. This species is believed to arise via a rapid 1,2-hydrogen atom shift reaction of the initial amidyl radical (Scheme 1). This novel shift reaction is analogous to the well-established 1,2-hydrogen atom shift reactions detected with alkoxyl and aminyl radicals, which occur in aqueous or alcoholic solution, but not organic solvents, as a result of the participation of a solvent −OH group in the transition state.[51,52] Similar C-2 carbon-centered radicals were detected on decomposition of the chloramides from di-*N*-acetyl chitobiose, tri-*N*-acetyl chitotriose, hexa-*N*-acetyl chitohexaose, *N*-acetyl allolactosamine, and some, but not all, of the alkyl glycosides.

Scheme 1. Formation of the *N*-Acetyl Glucosamine C-2 Carbon-Centered Radical via a Solvent-Assisted Amidyl 1,2-Hydrogen Shift

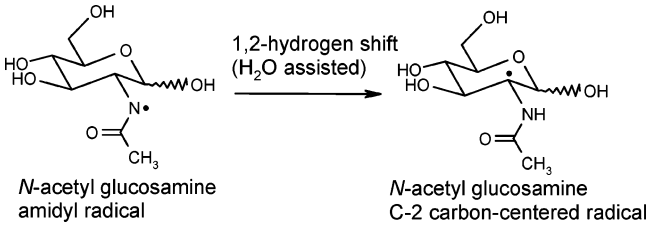

The ratio of the three isomeric MNP adducts of the *N*-acetyl glucosamine C-2 carbon-centered radical changed dramatically with increasing incubation time while the total adduct concentration remained relatively constant (Figure 2G). This is consistent with interconversion between these adducts. The signals are therefore assigned to two anomeric C-2 radical adducts, plus a third adduct species that could either be the open-chain form or a second conformer of one of the anomers. As the open-chain form would only be expected to be present at low concentrations, the second interpretation is favored. These adducts would be expected to undergo slow interconversion via mutarotation as observed with the parent compounds.[53] Similar effects were observed with both spin traps, and analogous behavior was observed with the C-2 carbon-centered radical MNP adducts detected from 2-acetamido-2-deoxy-3-*O*-methyl-D-glucopyranoside, *N*-acetyl allolactosamine, di-*N*-acetyl chitobiose, tri-*N*-acetyl chitotriose, and hexa-*N*-acetyl chitohexaose. This behavior suggests that the radicals detected are located on the reducing *N*-acetyl glucosamine residues. Such behavior was not detected with the corresponding glycosides that cannot undergo mutarotation.

The additional, or alternative, signals detected with the C-1 alkyl glycosides (β-methyl-, α-methyl-, β-ethyl-, β-isopropyl-, β-*tert*-butyl-) glycosides have been assigned to species formed via hydrogen atom abstraction from the alkyl group as a result of intramolecular 1,5- and 1,6-hydrogen shifts. In the case of the β-*tert*-butyl glycoside a 1,5-hydrogen shift to the glycosidic group cannot occur, and only radicals arising from a 1,2-hydrogen shift were observed. With 2-acetamido-2-deoxy-3-*O*-methyl-D-glucopyranoside a 1,5-hydrogen shift to the glycosidic group may occur; however, only C-2 carbon-centered radical adducts resulting from a 1,2-hydrogen shift were observed. The comparative rates of these competing rearrangement reactions cannot be determined from the EPR data as the observed adduct concentrations will depend on both the rate of rearrangement and the rate of radical trapping, with both of these unknown. However, with the β-ethyl and β-isopropyl species, the adducts arising from the 1,5-shift reaction predominate over those from the 1,2-reaction, as might be expected on the basis of the increasing stability of the incipient alkyl radical (second-

(47) Kochi, J. K. In *Free Radicals*; Kochi, J. K., Ed.; John Wiley and Sons: New York, 1973; Vol. 1, pp 591−683.
(48) Cotton, F. A.; Wilkinson, G. *Advanced Inorganic Chemistry*; John Wiley and Sons: New York, 1972.
(49) Marx, G.; Chevion, M. *Biochem. J.* **1986**, *236*, 397−400.
(50) Rees, M. D.; Hawkins, C. L.; Davies, M. J. Unpublished data.
(51) Gilbert, B. C.; Holmes, R. G. G.; Laue, H. A. H.; Norman, R. O. C. *J. Chem. Soc., Perkin Trans. 2* **1976**, 1047−1052.
(52) Elford, P. E.; Roberts, B. P. *J. Chem. Soc., Perkin Trans. 2* **1996**, 2247−2256.
(53) Angyal, S. J. *Adv. Carbohydr. Chem. Biochem.* **1991**, *49*, 19−35.

Scheme 2. Possible 1,5-Hydrogen Shift Reactions of Glycosaminoglycan Amidyl Radicals (Hyaluronan-Derived Radicals Shown)[a]

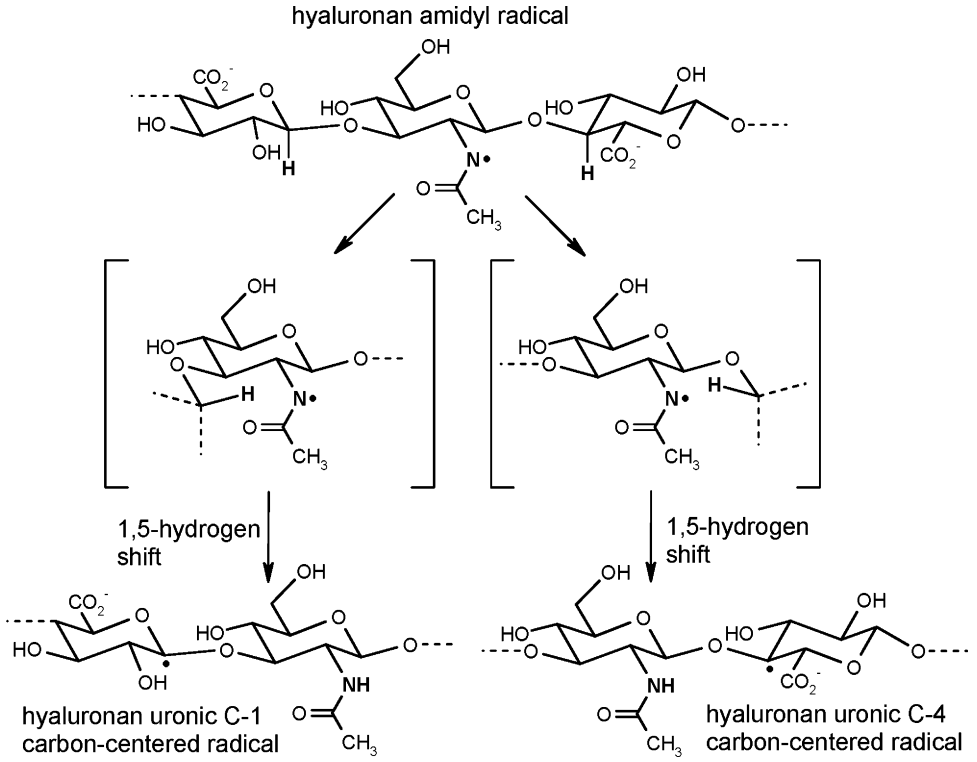

[a] Extensions of the partial structures shown are indicated by dashed bonds.

ary and tertiary alkyl-substituted species respectively). With the β-isopropyl glycoside, the most appropriate model for the polymers, the 1,5-shift predominates, although weak signals assigned to a primary alkyl radical resulting from a 1,6-hydrogen shift were also detected (molecular models suggest such a rearrangement would not occur with glycosaminoglycan-derived amidyl radicals). The DMPO adducts detected from the alkyl glycosides are assigned to the alkyl radicals formed on the glycosidic group, as the C-2 species is trapped inefficiently by DMPO, when compared to MNP, possibly as a result of steric hindrance. This is in accord with previous kinetic data.[54,55]

Molecular models of the glycosaminoglycans suggest that two alternative intramolecular 1,5-hydrogen atom abstraction reactions could occur with amidyl radicals formed on nonreducing (midchain) *N*-acetyl glycosamine residues to give carbon-centered radicals at C-1 and C-4 on the adjacent uronic acid residues (Scheme 2). In contrast, amidyl radicals formed on the nonreducing residues of the chitin oligosaccharides can only undergo a single 1,5-hydrogen atom abstraction reaction which generates a C-4 carbon-centered radical on adjacent *N*-acetyl glucosamine residues (Scheme 3). With amidyl radicals generated on the reducing residues of these oligosaccharides, no equivalent 1,5-hydrogen shift is possible. Consistent with this, a 1,2-hydrogen shift that generates a C-2 carbon-centered radical on the reducing residue appears to be the favored reaction of these amidyl radicals. The aforementioned 1,5-hydrogen shifts are postulated to be the source of the tertiary carbon-centered radicals detected with the glycosaminoglycans and chitin

Scheme 3. Possible 1,5-Hydrogen Shift Reaction of Chitin Oligosaccharide Amidyl Radicals Located on Nonreducing Residues[a]

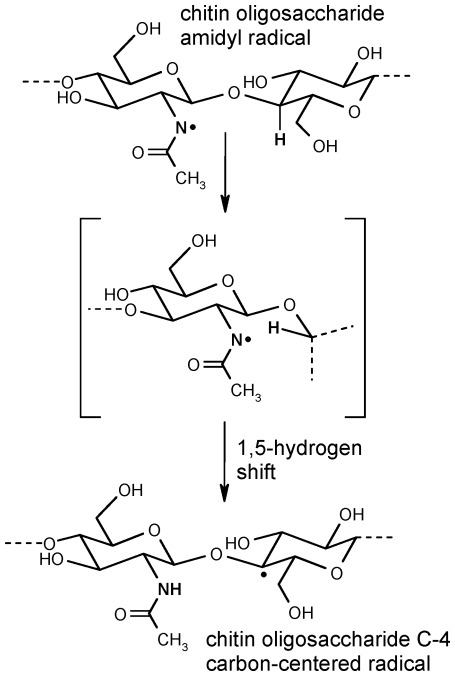

[a] Extensions of the partial structures shown are indicated by dashed bonds.

oligosaccharides, although in the case of the glycosaminoglycans, the data do not allow firm conclusions to be made as to whether only one, or both, possible rearrangements occur. However, the data obtained with 2-acetamido-2-deoxy-3-*O*-methyl-D-glucopyranoside suggests that reaction to give the C-4 uronic acid species is preferred (i.e. the right-hand reaction in

(54) Davies, M. J.; Timmins, G. S. In *Biomedical Applications of Spectroscopy*; Clark, R. J. H., Hester, R. E., Eds.; John Wiley & Sons Ltd: Chichester, 1996.
(55) Madden, K. P.; Taniguchi, H. *J. Chem. Soc., Perkin Trans. 2* **1993**, 2095−2103.

Scheme 4. Radical Reactions and Rearrangements Proposed To Be Consequent upon the Formation of Glycosaminoglycan Uronic C-4 Carbon-Centered Radicals (Hyaluronan-Derived Species Shown)[a]

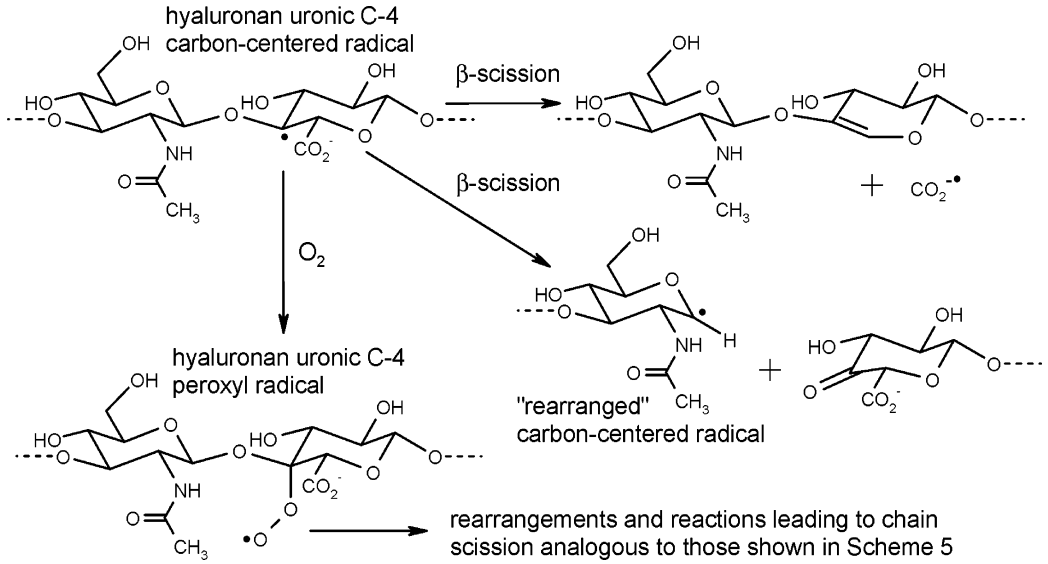

[a] Extensions of the partial structures shown are indicated by dashed bonds.

Scheme 2). Further support for the formation of the C-4 uronic acid species also arises from the detection of the DMPO adduct of $CO_2^{\bullet-}$, which is a likely β-scission product of these radicals (Scheme 5; cf. related β-scission reactions which yield this radical[56,57]).

With chondroitin-4-sulfate, hyaluronan, and the chitin oligosaccharides, there is only one site on these materials at which hydrogen atom abstraction can produce radicals with the partial structure •CHRR′: the $-CH_2-OH$ functions at the C-6 positions of *N*-acetyl glycosamine residues. However, it is unlikely that reaction at these sites would occur either intermolecularly (given the evidence already presented which suggests that intermolecular abstraction reactions by glycosamine-derived amidyl radicals are unimportant under the conditions employed) or intramolecularly (given the predicted stereochemical constraints on such reactions and the likely favorability of the aforementioned 1,5-hydrogen shifts: see above). Consequently, the •CHRR′ radicals assigned to species formed from further rearrangement of the initial carbon-centered species. The hyperfine coupling constants of adducts of the •CHRR′ radicals detected with the glycosaminoglycans and the chitin oligosaccharides are very similar (Table 1, cf. Figure 4, E and F), implying that these radicals are structurally similar. The formation of the chitin oligosaccharide •CHRR′ radicals is attributed to β-scission of the C-4 carbon-centered radicals formed via 1,5-hydrogen shifts to amidyl radicals located on nonreducing residues (cf. Scheme 3). The •CHRR′ radicals generated in this process are nearly identical (in terms of their local structure) to the •CHRR′ radicals which would be yielded upon β-scission of glycosaminoglycan-derived uronic acid C-4 carbon-centered radicals (Scheme 4).

Overall, the EPR data, and particularly that from the β-isopropyl glycoside and the chitin oligosaccharides, suggest that hydrogen-atom abstraction by an initial amidyl radical formed on the *N*-acetyl glycosamine ring of the glycosaminoglycans results predominantly in the formation of a C-4 carbon-centered radicals on the neighboring uronic acid residue via a 1,5-hydrogen atom shift. β-Scission of C-4 uronic acid radical would give strand scission and the observed •CHRR′ radicals (Scheme 4). This process is believed to be the major source of strand breaks with low O_2 concentrations.

The quantitative significance of these processes has been assessed with the C-1 alkyl glycosides where the alkyl group is converted into the corresponding carbonyl as a result of the reactions outlined in Scheme 5. These products are formed in high yield from the initial chloramide (Figure 5; $\leq$100% in the absence of O_2, ca. 50% in its presence), consistent with these reactions being facile and rapid. Analogous alkoxyl radical fragmentation reactions have been shown to increase in rate with increased steric crowding (due to the relief of strain), the stability of the resulting aldehyde/ketone, and the stabilization of the incipient radical center by the neighboring oxygen atoms. Each of these factors is likely to contribute positively to rapid fragmentation of the C-4 species located on the polymers and the chitin oligosaccharides. The detection of *N*-acetyl glucosamine (by HPLC) on decomposition of the alkyl glycoside chloramides is consistent with this process and subsequent oxidation/hydration of the resulting C-1 carbon-centered species.

Previous studies on the radiolytic oxidation of cellobiose have proposed that glycosidic bond cleavage in aqueous solution at neutral pH occurs via the formation of C-4-derived carbon-centered radicals adjacent to the lactol bridge, with subsequent chain scission via hydrolysis, rather than β-scission.[58] This conclusion was based on the assumption that C-1 carbon-centered radicals would not oxidize/hydrate to yield the corresponding reducing sugar, which was detected in high yield, under the conditions employed.[58] Although the rearranged radicals (•CHRR′) detected in the current study from chondroitin-4-sulfate, hyaluronan, and the chitin oligosaccharides could be due to carbonyl-conjugated radicals (e.g., •CHC(O)R) generated via acid- or base-catalyzed rearrangement of the C-4-derived α-hydroxyalkyl carbon-centered radicals released upon

(56) Davies, M. J.; Fu, S.; Dean, R. T. *Biochem. J.* **1995**, *305*, 643−649.
(57) Davies, M. J. *Arch. Biochem. Biophys.* **1996**, *336*, 163−172.
(58) von Sonntag, C.; Dizdaroglu, M.; Schulte-Frohlinde, D. *Z. Naturforsch.* **1976**, 857−864.

Scheme 5. Radical Reactions and Rearrangements Proposed To Be Consequent upon Formation of Glycosidic Carbon-Centered Radicals Adjacent to the Lactol Bridge on C-1 Alkyl Glycoside Derivatives; Such Species Are Analogous to Glycosaminoglycan Uronic C-4 Carbon-Centered Radicals (See Scheme 3)

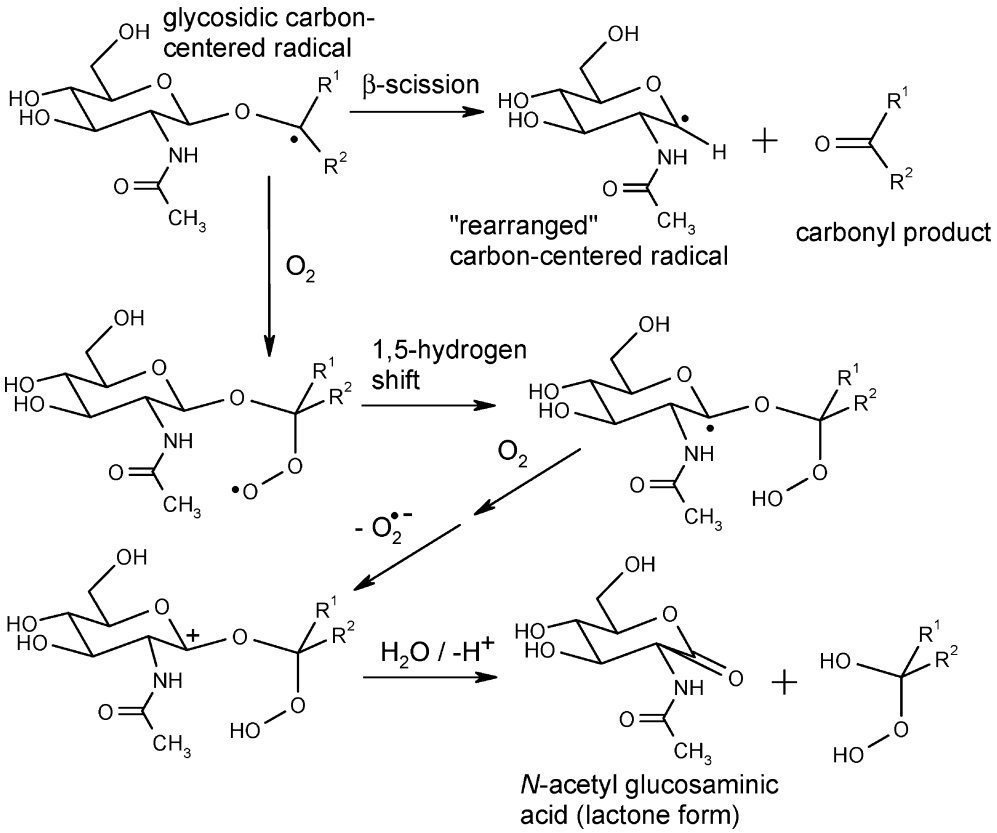

hydrolysis,[58,59] the detection of this species in high yields at pH 7.4 and pH 8.5 but not pH 5.5[50] is inconsistent with such an assignment. The current data is therefore consistent with the occurrence of two competing processes: a pH-independent β-scission pathway which gives rise to the rearranged species detected in the current study and, second, an acid-catalyzed process predominant at pH < 7.4 which gives rise to alternative (undetected) species via the hydrolytic mechanism proposed by von Sonntag;[58] the latter process may contribute to polymer fragmentation at low pH values.

The lower yields of products detected in the presence of O_2 have been ascribed to alternative pathways involving the formation of α-alkoxyalkyl peroxyl radicals on the glycosidic alkyl group; such species are analogous to glycosaminglycan uronic acid C-4 peroxyl radicals believed to be generated upon decomposition of glycosaminoglycan chloramides under aerobic conditions. These peroxyl radicals may also give rise to glycosidic bond scission via the reactions shown in Scheme 5, which is based on the behavior of α-alkoxyalkyl peroxyl radicals generated during the radiolysis of simple ethers.[60,61] With the C-1 alkyl glycoside derivatives, the occurrence of such reactions could account for the fact that the unidentified product detected in the gel chromatography studies with a retention time of 11.2 min was formed at the apparent expense of *N*-acetyl glucosamine in the presence of O_2 (Figure 5, Panels E−G: compare traces g and h in each case); this unidentified product is believed to be *N*-acetyl glucosaminic acid (cf. Scheme 4).

Decomposition of the β-ethyl-, β-isopropyl-, and β-*tert*-butyl glycosides yields methanal as a minor product in both the presence and absence of O_2, although in lower yield in the former case (Figure 5). This product is thought to arise via the formation of primary alkyl carbon-centered radicals ($^{\bullet}CH_2R$) via 1,6-hydrogen atom shift reactions. These reactions are less favorable than 1,5 reactions due to the larger ring size of the transition state.[38] Addition of O_2, and further reactions of the peroxyl radicals are the proposed source of the observed methanal (cf. data for other primary alkyl radicals[62]).

The alternative β-scission reaction of the C-4 uronic acid radical that generates $CO_2^{\bullet-}$ from the glycosaminoglycan chloramides may also ultimately lead to strand scission. This powerfully reducing radical[63] may redox cycle the transition metal ions that catalyze chloramide decomposition either directly or via the involvement of $O_2^{\bullet-}$, generated by reaction of O_2 with $CO_2^{\bullet-}$ (k ca. 2.5×10^9 dm^3 mol^{-1} s^{-1} [64]).

In the case of the glycosaminoglycans, the specific formation of C-4 uronic acid radicals and subsequent β-scission of these species is believed to be responsible for the regular bands detected on PAGE. The band spacing is identical to that detected for hyaluronidase enzymatic digests, implying cleavage at specific disaccharide repeats. The overall migration distance of the bands on the gel is, however, different to that induced by the enzymatic system, consistent with the presence of different end groups on the polymer fragments. This specific cleavage is in contrast to the essentially random damage induced by

(59) Davies, M. J.; Gilbert, B. C. *Adv. Detailed React. Mechs.* **1991**, *1*, 35−81.
(60) Schuchmann, M. N.; von Sonntag, C. *Z. Naturforsch.* **1986**, *42B*, 495−502.
(61) Schuchmann, M. N.; Schuchmann, H.-P..; von Sonntag, C. *J. Am. Chem. Soc.* **112**, 403−407.
(62) Schuchmann, M. N.; von Sonntag, C. *J. Phys. Chem.* **1982**, *86*, 1995−2000.
(63) Wardman, P. *J. Phys. Chem. Ref. Data* **1989**, *18*, 1637−1755.
(64) Neta, P.; Huie, R. E. *J. Phys. Chem. Ref. Data* **1988**, *17*, 1027−1284.

$HO^{\bullet}$.[65−67] The less specific banding observed in the presence of O_2 is consistent with the peroxyl radical reactions also resulting in strand cleavage.

The degradation of hyaluronan, chondroitin-4-sulfate, and (presumably) other *N*-acetylated glycosaminoglycans by myeloperoxidase-derived oxidants such as HOCl may be of considerable biological significance. It is well established that the extracellular matrix (ECM) plays a key role in modulating the behavior of cells including those of the vascular wall (reviewed in ref 19). Thus, the growth of bovine endothelial cells is modulated by different ECM substrata, and endothelial cell adhesion and proliferation is inhibited by matrix components (e.g. type V collagen) laid down by vascular smooth muscle cells.[68,69] Thus, (non-oxidized) matrix components can affect cellular adhesion and growth. Furthermore, human umbilical vein endothelial cells do not adhere readily to, or spread on, normal matrix materials that had been previously exposed to reagent HOCl or to a $MPO/H_2O_2/Cl^-$ system.[70] This has been ascribed to oxidative modification of matrix components including fibronectin, thrombospondin, and laminin.[71]

When compared to highly polymerized hyaluronan, which plays an important role in water homeostasis, plasma protein distribution, and matrix structure but is biologically relatively benign,[71] low-molecular-mass hyaluronan oligosaccharides have major biological effects. Hyaluronan fragments can induce macrophage expression of chemokines, cytokines, and growth factors (e.g., macrophage inflammatory protein-1α, macrophage inflammatory protein-1β, tumor necrosis factor-α, inducible nitric oxide synthase, plasminogen activator inhibitor-1, and macrophage metalloelastase) as well as up-regulation of a variety of cell-surface markers.[20−24] These processes are mediated, at least in part, via interferon-γ and NF-κB.[22] Oligomers of between 3 and 16 disaccharides have also been shown to stimulate angiogenesis in vivo and proliferation of cultured endothelial cells (but not fibroblast or smooth muscle cells)[25] although a recent report has reported that hyaluronan fragments stimulate VCAM-1 expression and the proliferation of cultured aortic smooth muscle cells, where the parent polymer has an inhibitory effect on proliferation.[72] Hyaluronan fragments also interact in an altered manner with the major cell-surface receptor for hyaluronan, CD44.[73]

Hyaluronan molecules of lower molecular mass accumulate at sites of inflammation and tissue injury[23,26−28] as do modified/fragmented versions of other matrix components including chondrotin sulfates.[29−31] These fragments may arise from the action of hyaluronidase,[33] which can be elevated at sites of disease,[73] although they may also potentially arise via the nonenzymatic, HOCl-mediated, processes outlined in the current study. As the oxidative fragments detected in the current study migrate on PAGE gels to a different extent than that of those generated enzymatically (cf. Figure 7), they are likely to be structurally distinct and have unique biological activities. The effects of these novel fragments are currently being studied.

Experimental Section

Reagents. Solutions were prepared using water filtered through a four-stage Milli Q system. pH control was achieved using 0.1 M phosphate buffer, pH 7.4, treated with washed Chelex resin (Bio-Rad, Hercules, CA) to remove contaminating trace metal ions. Adjustments to pH were made using 0.1 M monobasic sodium phosphate, 0.1 M dibasic sodium phosphate, or small quantities of concentrated perchloric acid or sodium hydroxide. In the case of the polymers, the addition of such solutions was achieved by buffer exchange using size-exclusion (PD10) chromatography (PD10 columns: Amersham Biosciences, Uppsula, Sweden). Chemicals were obtained from the following sources: sodium hyaluronate (hyaluronan) (120 kDa, Genzyme, Cambridge, MA); chondroitin sulfate A (chondroitin-4-sulfate) (whale cartilage, 25−50 kDa), *N*-acetyl allolactosamine, di-*N*-acetyl chitobiose, tri-*N*-acetyl chitotriose, and hexa-*N*-acetyl chitohexaose (Seikagaku, Tokyo, Japan); *N*-acetyl-D-glucosamine, methyl 2-deoxy-2-acetamido-β-D-glucopyranoside, methyl 2-deoxy-2-acetamido-α-D-glucopyranoside, and 2-acetamido-2-deoxy-3-*O*-methyl-D-glucopyranoside (Toronto Research Chemicals, North York, Ontario, Canada); *N*-acetyl-D-[2-^{13}C]-glucosamine and methyl 2-deoxy-2-acetamido-β-D-[2-^{13}C]-glucopyranoside (Omicron Biochemicals, South Bend, Indiana); ethyl 2-deoxy-2-acetamido-β-D-glucopyranoside, isopropyl 2-deoxy-2-acetamido-β-D-glucopyranoside, and *tert*-butyl 2-deoxy-2-acetamido-β-D-glucopyranoside (CMS Chemicals, Abingdon, Oxfordshire, UK). Myeloperoxidase (from human polymorphonuclear leukocytes) was obtained from Dr. C. Obinger, Institute of Chemistry, University of Agricultural Sciences, Wien, Austria. 5,5-Dimethyl-1-pyrroline *N*-oxide (DMPO; ICN, Seven Hills, NSW, Australia) was purified before use by treatment with activated charcoal. Stock solutions of 2-methyl-2-nitrosopropane (MNP) were made up in CH_3CN and diluted into the final reaction mixture such that the final concentration of CH_3CN was ≤10% v/v. HOCl solutions were prepared by dilution of a concentrated stock (0.5 M in 0.1 M NaOH) into 0.1 M, pH 7.4, phosphate buffer, with the HOCl concentration determined spectrophotometrically at pH 12 using ϵ_{292nm} 350 M^{-1} cm^{-1}.[2] All other chemicals were of analytical grade. Elimination of O_2 from reaction solutions was achieved by the use of nitrogen-saturated solutions and performing reactions in pre-sparged Pyrex HPLC vials (Chromacol, Trumbull, CT) sealed with Teflon septa. Liquid transfer to and from the reaction vessels was effected by gastight syringes.

Myeloperoxidase Incubations. Hyaluronan (3.65 mg/mL) or chondroitin-4-sulfate (4.6 mg/mL) and myeloperoxidase (1.25 μg/mL; ca. 20 nM in heme; ca. 0.11 units/mL by TNB method[75]) in chelex-treated phosphate buffered saline (100 mM NaCl, 100 mM phosphate, pH 7.4) were incubated at 37 °C for 5 min. While maintaining the solution at 37 °C, six aliquots of H_2O_2 (80 μM each) were added at 10 min intervals.[41] After further incubation at 37 °C for 10 min, the reaction was quenched by

(65) von Sonntag, C. *Adv. Carbohydr. Chem.* **1980**, *37*, 7−77.
(66) Parsons, B. J. In *Free Radical Damage and Control*; Rice-Evans, C. A., Burdon, R. H., Eds.; Elsevier Science: Amsterdam, 1994.
(67) Uchiyama, H.; Dobashi, Y.; Ohkouchi, K.; Nagasawa, K. *J. Biol. Chem.* **1990**, *265*, 7753−7759.
(68) Underwood, P. A.; Bennett, F. A. *Exp. Cell. Res.* **1993**, *205*, 311−319.
(69) Underwood, P. A.; Bean, P. A.; Whitelock, J. M. *Atherosclerosis* **1998**, *141*, 141−152.
(70) Vissers, M. C.; Thomas, C. *Free Radical Biol. Med.* **1997**, *23*, 401−411.
(71) Laurent, T. C.; Laurent, U. B.; Fraser, J. R. *Ann. Rheum. Dis.* **1995**, *54*, 429−432.
(72) Cuff, C. A.; Kothapalli, D.; Azonobi, I.; Chun, S.; Zhang, Y.; Belkin, R.; Yeh, C.; Secreto, A.; Assoian, R. K.; Rader, D. J.; Pure, E. *J. Clin. Invest.* **2001**, *108*, 1031−1040.
(73) Lesley, J.; Hascall, V. C.; Tammi, M.; Hyman, R. *J. Biol. Chem.* **2000**, *275*, 26967−26975.
(74) Lokeshwar, V. B.; Young, M. J.; Goudarzi, G.; Iida, N.; Yudin, A. I.; Cherr, G. N.; Selzer, M. G. *Cancer Res.* **1999**, *59*, 4464−4470.
(75) Kettle, A. J.; Winterbourn, C. C. *Methods Enzymol.* **1994**, *233*, 502−512.

isolating the high-molecular-mass species by size-exclusion (PD10) chromatography.

Enzymatic Digestion of Polymers. Hyaluronidase digests of chondroitin-4-sulfate and hyaluronan were prepared as described previously.[76] Chondroitin-4-sulfate (1.74 mg/mL) samples were incubated at 37 °C in saline/acetate buffer (0.15 M NaCl/0.1 M NaOAc, pH 5.0) with testicular hyaluronidase (196 units/mL) in the presence of 0.1% gelatin for 0.5, 1, 2, and 24 h. Reaction was terminated by incubation in boiling water for 10 min,and then the samples were stored at −18 °C until use. Additional aliquots of hyaluronidase (ca. 95 units/mL) were added after 1 and 2 h incubation in the 24 h digest and after 1 h in the 2 h digest. Hyaluronan (8.7 mg/mL) was incubated at 37 °C in saline acetate buffer (0.15 M NaCl/0.1 M NaOAc/ 0.001 M Na_2EDTA, pH 5.0) with testicular hyaluronidase (204 units/mL) in the presence of 0.1% gelatin. Separate digests were incubated for 1 and 2.5 h respectively, heated in boiling water for 10 min, and then stored at −18 °C until used. An additional aliquot of hyaluronidase (196 units/mL) was added after 1 h in the 2.5 h digest. The digests were diluted 10-fold before use.

UV−Visible Spectroscopy. UV−visible spectra were recorded on a Perkin-Elmer Lambda 40 spectrophotometer at 37 °C with the temperature maintained using a Peltier block. Spectra were acquired (relative to a 100 mM phosphate buffer baseline) between 220 and 400 nm (1 nm intervals) at 960 nm/ min with a time interval of 5−30 min, depending on the reaction time scale.

Assay of Chloramide Yields. 5-Thio-2-nitrobenzoic acid (TNB; 35−45 μM) was used to quantify the yield of *N*-chloro species after 15 min reaction at ca. 21 °C using ϵ_{412nm} 13 600 M^{-1} cm^{-1}.[40] None of the reagents employed interfered significantly with such measurements with the exception Cu^{2+} at concentrations >0.6 μM final concentration. Background values obtained in the presence of the metal ion, but absence of chloramide, were subtracted from the experimental data.

EPR Spectroscopy. EPR spectra were recorded at room temperature using a Bruker EMX X-band spectrometer with 100 kHz modulation and a cylindrical ER4103TM cavity. Samples were contained in a flattened, aqueous sample cell (WG-813-SQ; Wilmad, Buena, NJ), and spectral recording was initiated within 2 min of addition of the transition metal ions and/or spin trap. Sequential spectra were recorded for periods of up to 60 min. These experiments were performed on samples where all the HOCl was consumed, or removed, to avoid direct reaction of HOCl with DMPO;[77] the absence of HOCl in such solutions was established spectrophotometrically. Hyperfine couplings were measured directly from the field scan and confirmed by computer simulation using the program WINSIM (available at http://EPR.niehs.nih.gov). Correlation coefficients between simulated and experimental spectra were >0.95. Typical EPR spectrometer settings were: gain, 1×10^5; modulation amplitude 0.01−0.02 mT; time constant, 0.16 s; scan time, 84 s; resolution 1024 points; center field, 384 mT; field scan 6.5−10 mT; power, 25 mW; frequency, 9.76 GHz; with 2−8 scans averaged.

Carbonyl Quantification. Methanal, ethanal, and propan-2-one were quantified by conversion to the corresponding hydrazones by reaction (1:1 v/v) with 2,4-dinitrophenylhydrazine (DNPH; 10 mM in CH_3CN) at ca. 21 °C for 16 h.[78] Separation of the hydrazones was achieved by HPLC using a 5 μm C18 ODS column (Zorbax, Agilent Technologies, Forest Hill, VIC, Australia). Samples (10 μL) were eluted at 30 °C at a flow rate of 1.0 mL/min using the following stepwise gradient: 0−10 min 55.6% solvent B; 10.1−30 min 88.9% solvent B; 30.1−35 min 100% solvent B; 35.1−45 min equilibration to initial conditions, where solvent A was 10% (v/v) methanol in water and solvent B was 10% (v/v) methanol in acetonitrile. Solvents were filtered prior to use using 0.2 μm Supor Membrane filters (Gelman Laboratories, Ann Arbor, MI) and bubbled with helium. The hydrazones were detected by UV absorbance at 365 nm and quantified using standards.

Gel Permeation/Ligand-Exchange Chromatography. Samples were filtered (0.45-μm pore size filter; Nanosep MF GHP; Pall Life Sciences, Ann Arbor, MI) then analyzed by HPLC using a Shodex Ionpak KS-803 column (8 × 300 mm; sulfonated polystyrene−divinylbenzene copolymer strong cation-exchange gel; exclusion limit 50 kDa) with a Shodex Ionpak KS-G guard column (6 × 50 mm; Showa Denko, Tokyo, Japan). Samples (10 μL) were eluted at 70 °C at a flow rate of 0.7 mL/min using 50 mM NaCl as eluent. The eluent was monitored spectrophotometrically (190−370 nm) using a SPD-10A*vp* UV−vis detector (Shimadzu, Kyoto, Japan).

Polyacrylamide Gel Electrophoresis. Samples were analyzed using 20 or 30% polyacrylamide gels (0.1 cm × 16 cm × 20 cm, Protean II xi system, Bio-Rad Laboratories, Hercules, CA).[43] Aliquots (40 μL) from reaction mixtures were treated with 5 μL of 200 mM methionine at room temperature for 30 min to quench residual chloramides, then stored at −18 °C prior to analysis. 1 M Tris/0.25 M borate/0.01 M EDTA buffer pH 8.3 (10 × TBE buffer) containing 2 M sucrose (10 μL) was added to 45 μL of sample, with 50 μL (10−20 μL where silver staining was employed) then loaded onto 20 or 30% polyacrylamide gels with 1 × TBE used as running buffer. Twenty percent gels were run at 75 V (chondroitin-4-sulfate samples) or 120 V (hyaluronan samples) for 15 h at room temperature. Thirty percent gels were run at 200 V (chondroitin-4-sulfate samples) or 300 V (hyaluronan samples) for 24 h at 10 °C using water as coolant. Glycosaminoglycans were visualized by staining with 0.5% Alcian Blue in 2% CH_3COOH[76] or by using a combined Alcian Blue/silver staining method.[79] Gels were scanned and digitized over a linear range using a Bio-Rad Gel Doc 1000 system and software (Bio-Rad, Hercules, CA).

Acknowledgment. We thank the Australian Research Council and the National Health and Medical Research Council for financial support. MR gratefully acknowledges the award of an Australian Postgraduate Award administered through the University of Sydney.

Supporting Information Available: Two tables containing hyperfine coupling constants of spin adduct data obtained using MNP (Table 1) and DMPO (Table 2) as spin traps (PDF). This material is available free of charge via the Internet at http://pubs.acs.org.

JA0370591

(76) Turner, R. E.; Cowman, M. K. *Arch. Biochem. Biophys.* **1985**, *237*, 253−260.
(77) Bernofsky, C.; Bandara, B. M.; Hinojosa, O. *Free Radical Biol. Med.* **1990**, *8*, 231−239.
(78) Headlam, H. A.; Davies, M. J. *Free Radical Biol. Med.* **2002**, *32*, 1171−1184.
(79) Min, H.; Cowman, M. K. *Anal. Biochem.* **1986**, *155*, 275−285.